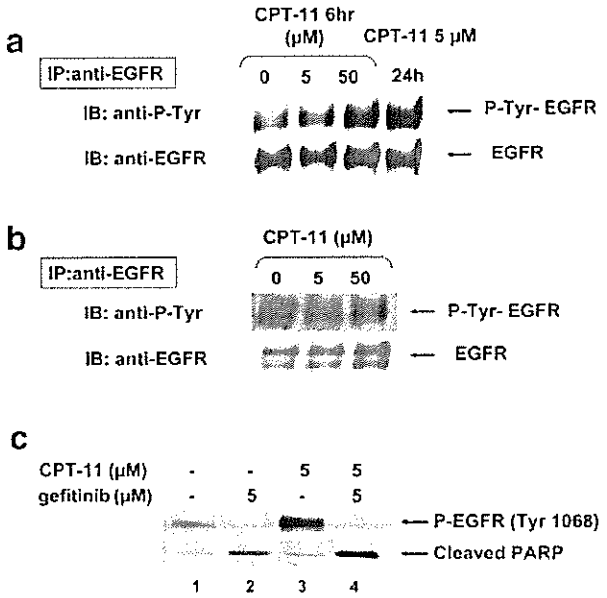


FIGURE 5 – The effect of CPT-11 on EGFR phosphorylation in WiDR cells. Lovo (*a*) and WiDR (*b*) cells ($5\times10^6$) were treated with 5 or 50 μM CPT-11 for 6 hr. Additionally Lovo cells were treated with 5 μM CPT-11 for 24 hr. The 1,500 μg of total cell lysate was immunoprecipitated with an anti-EGFR antibody. Tyrosine-phosphorylated EGFR was determined with an anti-phosphotyrosine antibody and the membranes were reblotted by anti-EGFR antibody. (*c*) Lovo cells were treated with gefitinib or CPT-11 alone (lane 2 and 3) and in combination (lane 4) for 24 hr. A 20 μg of protein of each sample was analyzed by Western blotting using antiphospo-EGFR (Tyr 1068) and cleaved PARP antibody.

drugs. These results suggest that this regimen is intensive but can be tolerated, at least in mice.

The *in vitro* and *in vivo* experiments in our study demonstrated the synergistic potential of gefitinib – CPT-11 combination. We previously reported that topoisomerase I up-regulation by counter-part drugs was a possible mechanism for the synergy in an CPT-11 containing regimen.[23] On the other hand, the synergistic potential of gefitinib with topotecan, cisplatin, paclitaxel or radiation has been reported.[18,24–28] To elucidate the biochemical mechanism underlying the synergistic interaction between the gefitinib and CPT-11, the effect of CPT-11 on EGFR-phosphorylation was examined (Fig. 5). Increased phosphorylation of EGFR was observed after exposure to CPT-11 in dose and time-dependent manner in WiDR and Lovo cells. Since EGFR expression and phosphorylation were the major determining factors for sensitivity of the cells to gefitinib-induced growth-inhibition,[14] biochemical modulation of EGFR by CPT-11 might be responsible for the synergistic interaction between gefitinib and CPT-11. EGFR is induced and activated by cellular stress, such as oxidative stress and UV irradiation.[29–34] Ohmori *et al.*[22] demonstrated that increased autophosphorylation of EGFR was obtained in cisplatin-exposure in human lung cancer cells. A number of reports suggest that EGFR promotes cell survival through the activation of the ERK or the AKT pathway.[31,32] EGFR activation induced by these cellular stress may play a survival response against apoptosis.[31,32] In the present study, PARP activation by gefitinib was markedly enhanced by combination with CPT-11 at 5 μM exposure, which is comparable with $IC_{50}$ value of CPT-11 in Lovo cells, although no PARP activation was observed by monotherapy of CPT-11. On the other hand, gefitinib does not modify the expression and the activation of topoisoerase I (data not shown). These result suggest that the inhibitory effect of gefitinib on the activated survival signal transduction induced by CPT-11 lead to synergistic effect. The findings of the present study suggest that biological modulation by various anticancer agents including DNA damaging agents will contribute to the synergistic effects of these anticancer agents and gefitinib in EGFR expressing tumor and support clinical evaluation of gefitinib in combination with DNA-targeting agents, especially CPT-11, in the treatment of colorectal cancers.

## REFERENCES


1. Blijham G, Wagener T, Wils J, de Greve J, Buset M, Bleiberg H, Lacave A, Dalmark M, Selleslag J, Collette L, Sahmoud T. Modulation of high-dose infusional fluorouracil by low-dose methotrexate in patients with advanced or metastatic colorectal cancer: final results of a randomized European Organization for Research and Treatment of Cancer Study. J Clin Oncol 1996;14:2266–73.
2. O'Connell MJ, Klaassen DJ, Everson LK, Cullinan S, Wieand HS. Clinical studies of biochemical modulation of 5-fluorouracil by leucovorin in patients with advanced colorectal cancer by the North Central Cancer Treatment Group and Mayo Clinic. NCI Monogr 1987;185–8.
3. Focan C, Kreutz F, Focan-Henrard D, Moeneclaey N. Chronotherapy with 5-fluorouracil, folinic acid and carboplatin for metastatic colorectal cancer; an interesting therapeutic index in a phase II trial. Eur J Cancer 2000;36:341–7.
4. Shimada Y, Yoshino M, Wakui A, Nakao I, Futatsuki K, Sakata Y, Kambe M, Taguchi T, Ogawa N. Phase II study of CPT-11, a new camptothecin derivative, in metastatic colorectal cancer. CPT-11 Gastrointestinal Cancer Study Group. J Clin Oncol 1993;11:909–13.
5. Cunningham D, Pyrhonen S, James RD, Punt CJ, Hickish TF, Heikkila R, Johannesen TB, Starkhammar H, Topham CA, Awad L, Jacques C, Herait P. Randomised trial of irinotecan plus supportive care versus supportive care alone after fluorouracil failure for patients with metastatic colorectal cancer. Lancet 1998;352:1413–8.
6. Saltz LB, Cox JV, Blanke C, Rosen LS, Fehrenbacher L, Moore MJ, Maroun JA, Ackland SP, Locker PK, Pirotta N, Elfring GL, Miller LL. Irinotecan plus fluorouracil and leucovorin for metastatic colorectal cancer: Irinotecan Study Group. N Engl J Med 2000;343:905–14.
7. Rothenberg ML, Meropol NJ, Poplin EA, Van Cutsem E, Wadler S. Mortality associated with irinotecan plus bolus fluorouracil/leucovorin: summary findings of an independent panel. J Clin Oncol 2001;19:3801–7.
8. Modi S. Seidman AD. An update on epidermal growth factor receptor inhibitors. Curr Oncol Rep 2002;4:47–55.
9. Saijo N, Tamura T, Nishio K. Problems in the development of target-based drugs. Cancer Chemother Pharmacol 2000;46:S43–5.
10. Baselga J. The EGFR as a target for anticancer therapy: focus on cetuximab. Eur J Cancer 2001;37:S16–22.
11. Nicholson RI, Gee JM, Harper ME. EGFR and cancer prognosis. Eur J Cancer 2001;37:S9–15.
12. Speer G, Cseh K, Winkler G, Takacs I, Barna I, Nagy Z, Lakatos P. Oestrogen and vitamin D receptor (VDR) genotypes and the expression of ErbB-2 and EGF receptor in human rectal cancers. Eur J Cancer 2001;37:1463–8.
13. Albanell J, Rojo F, Baselga J. Pharmacodynamic studies with the epidermal growth factor receptor tyrosine kinase inhibitor ZD1839. Semin Oncol 2001;5:56–66.
14. Mendelsohn J, Baselga J. The EGF receptor family as targets for cancer therapy. Oncogene 2000;19:6550–65.
15. Woodburn JR, Morris CQ, Kelly H. EGF receptor tyrosine kinase inhibitors as anti-cancer agents-preclinical and early clinical profile of ZD1839. Cell Mol Biol Lett 1998;3:348–9.
16. Naruse I, Ohmori T, Ao Y, Fukumoto H, Kuroki T, Mori M, Saijo N, Nishio K. Antitumor activity of the selective epidermal growth factor receptor-tyrosine kinase inhibitor (EGFR-TKI) Iressa™ (ZD1839) in a EGFR-expressing multidrug resistant cell line in vitro and in vivo. Int J Cancer 2002;98:310–5.
17. Ciardiello F, Bianco R, Damiano V, De Lorenzo S, Pepe S, De Placido S, Fan Z, Mendelsohn J, Bianco AR, Tortora G. Antitumor activity of sequential treatment with topotecan and anti-epidermal

growth factor receptor monoclonal antibody C225. Clin Cancer Res 1999;5:909–16.
18. Ciardiello F, Caputo R, Bianco R, Damiano V, Pomatico G, De Placido S, Bianco A.R, Tortora G. Antitumor effect and potentiation of cytotoxic drugs activity in human cancer cells by ZD-1839 (Iressa), an epidermal growth factor receptor-selective tyrosine kinase inhibitor. Clin Cancer Res 2000;6:2053–63.
19. Sirotnak FM, Zakowski MF, Miller VA, Scher HI, Kris MG. Efficacy of cytotoxic agents against human tumor xenografts is markedly enhanced by coadministration of ZD1839 (Iressa), an inhibitor of EGFR tyrosine kinase. Clin Cancer Res 2000;6:4885–92.
20. Slichenmyer WJ, Fry DW. Anticancer therapy targeting the erbB family of receptor tyrosine kinases. Semin Oncol 2001;28:67–79.
21. Kusaba H, Tamura T, Nakagawa K, Yamamoto N, Kudoh S, Negoro S, Takeda K, Tanigawara Y, Fukuoka M. A phase I intermittent dose-escalation trial of ZD1839 ('IRESSA') in Japanese patients with solid malignant tumors. Clin Cancer Res 2000;6:abs381.
22. Kris M, Ranson M, Ferry D, Hammond L, Averbuch S, Ochs J, Rowinsky E. Phase I study of oral ZD1839('IRESSA'): A novel inhibitor of epidermal growth factor receptor tyrosine kinase (EGFR-TKI)—Evidence of good tolerability and activity. Clin Cancer Res 1999;5:abs 99
23. Kanzawa F, Koizumi F, Koh Y, Nakamura T, Tatsumi Y, Fukumoto H, Saijo N, Yoshioka T, Nishio K. In vitro synergistic interactions between the cisplatin analogue nedaplatin and the DNA topoisomerase I inhibitor irinotecan and the mechanism of this interaction. Clin Cancer Res 2001;7:202–9.
24. Ohmori T, Ao Y, Nishio K, Saijo N, Arteaga CL, Kuroki T. Low dose cisplatin can modulate the sensitivity of human non-small cell lung carcinoma cells to EGFR tyrosine kinase inhibitor (ZD1839; 'Iressa') in vivo. Proc Am Assoc Cancer Res 2000;41:abs 3072.
25. Magne N, Fischel JL, Dubreuil A, Formento P, Marcie S, Lagrange JL, Milano G. Sequence-dependent effects of ZD1839 ('Iressa') in combination with cytotoxic treatment in human head and neck cancer. Br J Cancer 2002;86: 819–27.
26. Raben D, Helfrich BA, Chan D, Johnson G, Bunn PA Jr. ZD1839, a selective epidermal growth factor receptor tyrosine kinase inhibitor, alone and in combination with radiation and chemotherapy as a new therapeutic strategy in non-small cell lung cancer. Semin Oncol 2002; 29:37–46.
27. Sirotnak FM, Zakowski MF, Miller VA, Scher HI, Kris MG. Efficacy of cytotoxic agents against human tumor xenografts is markedly enhanced by coadministration of ZD1839 (Iressa), an inhibitor of EGFR tyrosine kinase. Clin Cancer Res 2000;6:4885–92.
28. Williams KJ, Telfer BA, Stratford IJ, Wedge SR. ZD1839 ('Iressa'), a specific oral epidermal growth factor receptor-tyrosine kinase inhibitor, potentiates radiotherapy in a human colorectal cancer xenograft model. Br J Cancer 2002;86:1157–61.
29. Goldshmit Y, Erlich S, Pinkas-Kramarski R. Neuregulin rescues PC12-ErbB4 cells from cell death induced by $H_2O_2$. Regulation of reactive oxygen species levels by phosphatidylinositol 3-kinase. J Biol Chem 2001;276:46379–85.
30. Meves A, Stock SN, Beyerle A, Pittelkow MR, Peus D. $H_2O_2$ mediates oxidative stress-induced epidermal growth factor receptor phosphorylation. Toxicol Lett 2001;122:205–14.
31. Miyazaki Y, Hiraoka S, Tsutsui S, Kitamura S, Shinomura Y, Matsuzawa Y. Epidermal growth factor receptor mediates stress-induced expression of its ligands in rat gastric epithelial cells. Gastroenterology 2001;120:108–16.
32. Wang X, McCullough KD, Franke TF, Holbrook NJ. Epidermal growth factor receptor-dependent Akt activation by oxidative stress enhances cell survival. J Biol Chem 2000;275:14624–31.
33. Benhar M, Engelberg D, Levitzki A. Cisplatin-induced activation of the EGF receptor. Oncogene 2002;21:8723–31.
34. Kitagawa D, Tanemura S, Ohata S, Shimizu N, Seo J, Nishitai G, Watanabe T, Nakagawa K, Kishimoto H, Wada T, Tezuka T, Yamamoto T, et al. Activation of extracellular signal-regulated kinase by ultraviolet is mediated through Src-dependent epidermal growth factor receptor phosphorylation: its implication in an anti-apoptotic function. J Biol Chem 2002;277:366–71.

*Nucleosides, Nucleotides, and Nucleic Acids*, 25:647–654, 2006

ISSN: 1525-7770 print / 1532-2335 online
DOI: 10.1080/15257770600686360

Taylor & Francis
Taylor & Francis Group

# SYNTHESIS AND BIOLOGICAL PROPERTIES OF NEW PHOSMIDOSINE ANALOGS HAVING AN *N*-ACYLSULFAMATE LINKAGE

**Haruhiko Taguchi, Akihiro Ohkubo, and Mitsuo Sekine** □ *Department of Life Science, Tokyo Institute of Technology, Nagatsuta, Midoriku, Yokohama, Japan, and CREST, JST (Japan Science and Technology Agency), Yokohama, Japan*

**Kohji Seio** □ *Frontier Collaborative Research Center, Tokyo Institute of Technology, Nagatsuta, Midoriku, Yokohama 226-8503, Japan, and CREST, JST (Japan Science and Technology Agency), Yokohama, Japan*

**Hideaki Kakeya and Hiroyuki Osada** □ *Discovery Research Institute, RIKEN, Wako, Saitama, Japan*

**Takuma Sasaki** □ *School of Pharmacy, Aichi Gakuin University, Nagoya, Japan*

□ *A new phosmidosine analog* **10**, *in which the proline and 8-oxoadenosine moieties were linked by an* N*-acyl sulfamate linkage, was successfully synthesized by the sulfamoylation of an 8-oxoadenosine derivative* **5** *followed by coupling with an* L*-proline derivative* **8**. *An* L*-alanine-substituted derivative* **13** *and its derivative* **14** *without the alanyl residue were also synthesized. The morphological reversion activity of these synthetic compounds in v-src*$^{ts}$ *NRK cells and their antitumor activity in L1210 and KB cells were studied. As the result, neither* L*-proline- nor* L*-alanine-substituted phosmidosine analogs* **10** *and* **13** *showed any antitumor activity. Contrary to these results, the derivative* **14** *lacking the amino acid residue showed potent antitumor activities against cancer cells.*

**Keywords** *N*-acyl sulfamate linkage; Phosmidosine analogs; Morphological reversion activity; Antitumor activity

Received 23 January 2006; accepted 21 February 2006.

This work was financially supported by CREST of JST (Japan Science and Technology Agency). This study was partially supported by Industrial Technology Research Grant Program in '05 from New Energy and Industrial Technology Development Organization (NEDO) of Japan. The authors would like to thank R. Onose for helpful assistance.

This article is dedicated to Professor Eiko Ohtsuka on the occasion of her 70th birthday.

Address correspondence to Haruhiko Taguchi. Department of Life Science, Tokyo Institute of Technology, Nagatsuta, Midoriku, Yokohama, 226-8501, Japan. E-mail: msekine@bio.titech.ac.jp

## INTRODUCTION

A number of artificial aminoacyl adenylate derivatives having an *N*-acylsulfamate linkage have been synthesized and their biological properties have been studied.[1–4] Alanyl-, arginyl-, prolyl-, and asparaginyl adenylate analogs were synthesized. The chemical stability of the *N*-acylsulfamate linkage of aminoacyl adenylate derivatives is higher than that of the corresponding *N*-acylphosphoramidate linkage under physiological conditions. Therefore, a series of aminoacyl adenylate analogs containing *N*-acylsulfamate linkages have been used as aminoacyl-tRNA synthetase inhibitors.[1–3] Nucleocidin, which has an *N*-acylsulfamate linkage lacking the aminoacyl residue, is known to be highly toxic and to act as a highly potent inhibitor of protein synthesis.[4,5] Ascamycin, which was isolated from *Xanthomonas spp.* in 1984,[6] is a nucleoside derivative possessing an *N*-acylsulfamate linkage and a 2-chloroadenine residue as the nucleobase. Isono et al. reported the biological properties of ascamycin and its analogs substituted with other amino acids, showing that these compounds have highly potent antibacterial activities.[7] They also reported that a dealanylascamycin called AT-256, which was produced by Xc-aminopeptidase-promoted hydrolysis of ascamycin,[8] inhibited protein synthesis. Aminoacyl adenylate derivatives having an *N*-acylphosphoramide linkage have also been studied and their chemical and biological properties have been clarified. The P–N bond of the *N*-acylphosphoramide linkage is more stable than the corresponding P–O bond of an *O*-acylphosphoramide linkage and these modified nucleosides showed antitumor activities. A naturally occurring antibiotic, phosmidosine, has proved to possess potent antitumor activities against various human cancer cells.[9–11] McCloskey reported that phosmidosine was decomposed by treatment with 0.2 M NaOH to produce a proline moiety-lacking compound and rearranged compounds.[12] Recently, we have studied the synthesis of phosmidosine and its analogs.[13–17] In our continuous studies of the structure-activity relationship of a series of phosmidosine derivatives, we found that the 8-oxoadenine base and the proline moiety were essential for inhibition of the cancer cell growth.[15] These results prompted us to synthesize new phosmidosine analogs having an *N*-acylsulfamate linkage.

## RESULTS AND DISCUSSION

A general procedure for construction of *N*-acylsulfamoyl linkage has been developed to obtain a series of aminoacyl adenylate derivatives containing an *N*-acylsulfamoyl linkage.[1–4] Therefore, we applied this method to the synthesis of our new phosmidosine analogs.

Thus, the *O*-selective reaction of an appropriately protected 8-oxoadenosine derivative 5 with sulfamoyl chloride,[2,18] which was prepared from chlorosulfonyl isocyanate and formic acid, was studied. As the result,

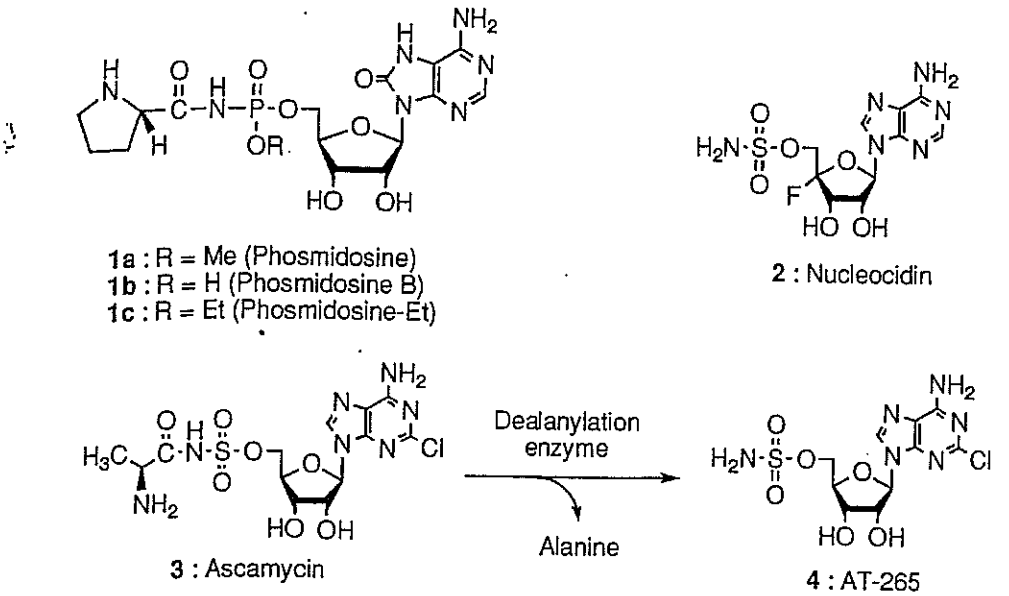


**FIGURE 1** Structure of several aminoacyl adenylate derivatives.

the desired sulfamoylation proceeded to afford the 5′-*O*-sulfamoyl-8-oxoadenosine derivative **6**. In this reaction, no reactions occurred on the 7-position or the 6-amino group of the 8-oxoadenine moiety. In an attempt to obtain an *N*-acyl sufamate derivative **9**, an L-proline derivative was activated by treatment with *N*, *N*′-carbonyldiimidazole and the resulting acylimidazole derivative **7** was allowed to react with **6**. However, no prolylated compounds were obtained. In contrast to this result, when the *O*-succsinyl-L-proline derivative **8**[2] was used, the reaction gave the desired product **9** in a moderate yield. The yield of **9** was increased to 80% by the choice of

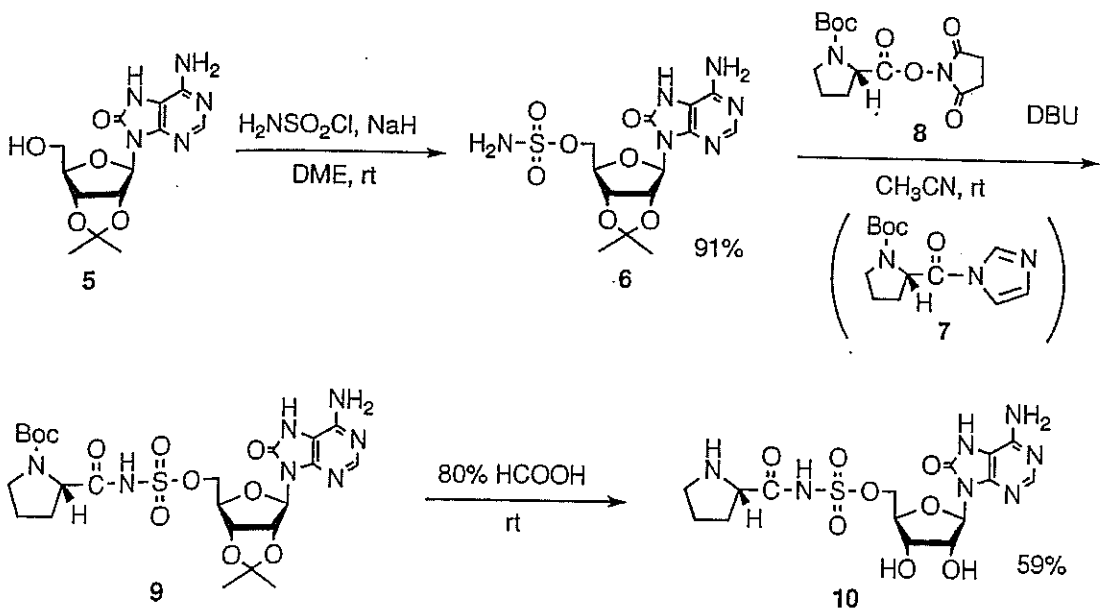


**FIGURE 2** Synthesis of phosmidosine analogs.

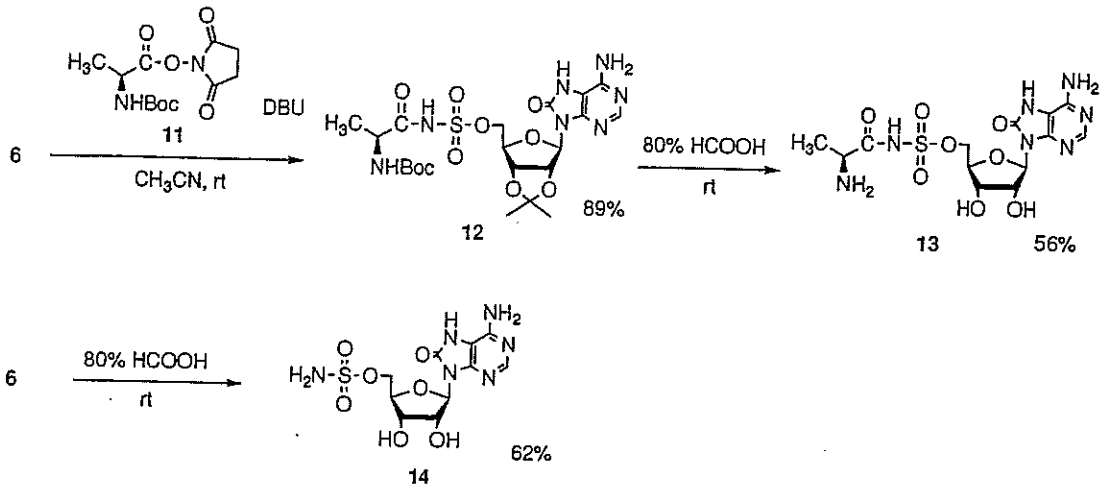


**FIGURE 3** Synthesis of ascamycin mimics.

acetonitrile as the solvent. The product was treated with 80% formic acid for 12 h to give the product **10** as an amorphous white solid in 59% yield.

In a similar manner, we also synthesized an ascamycin mimic **13**, which was obtained by the reaction of **6** with the ester **11** followed by acidic treatment of the product **12**. The compound **14**, which does not have the alanyl residue, was synthesized by treatment of **6** with 80% HCOOH.

The morphological reversion activity of these synthetic compounds in v-src$^{ts}$NRK cells and their antitumor acttivity in L1210 and KB cells were studied. These results are shown in Table 1.

**TABLE 1** The Biological Properties of Compounds **1c**, **10**, **13**, and **14**

| | Morphological reversion activity ($\mu$g/ml) | | | | | | |
|---|---|---|---|---|---|---|---|
| Aminoacyl nuclesides | 100 | 30 | 10 | 3 | 1 | 0.3 | 0.1 |
| Morphological reversion activity of phosmidosine analogs in v-src$^{ts}$ NRK cells | | | | | | | |
| L-Pro-Sulfamoyl-8-oxoA : **10** | − | − | − | − | − | − | − |
| H-Sulfamoyl-8-oxoA : **14** | +++ | +++ | +++ | +++ | + | − | − |
| Phosmidosine-Et : **1C** | nt | nt | +++ | +++ | + | nt | nt |

| | L1210 $\mu$M | KB $\mu$M |
|---|---|---|
| $IC_{50}$ Values of phosmidosine analogs in L1210 and KB cells | | |
| L-Pro-Sulfamoyl-8-oxoA : **10** | 218< | 218< |
| L-Ala-Sulfamoyl-8-oxoA : **13** | 231< | 231< |
| H-Sulfamoyl-8-oxoA : **14** | 0.91 | 4.86 |
| Phosmidosine-Et : **1C** | 3.62 | 3.44 |

+++:More than 75% of cancer cells were morphologically reversed.
++:25–75% of cancer cells were morphologically reversed.
+:ca. 25% oc cancer cells were morphologically reversed.
−:no activity; nt: not tested.

As shown in Table 1, the phosmidosine ethyl ester **1c** was used as a control sample. In the morphological reversion activity assay, the L-proline-substituted phosmidosine analog **10** did not show any morphological reversion activities. However, compound **14** showed morphological reversion activity at a low concentration. Even when the concentration was 3 $\mu$g/ml, morphological reversion activity was significantly observed. Next, we studied the antitumor activity of these compounds against L1210 and KB cells. The results were similar to those obtained in the case of the morphological reversion activity assay. Only compound **14** inhibited the growth of L1210 and KB cells. The structure of compound **14** is similar to those of nucleocidin **2** and AT-265 **4**.

In conclusion, we have successfully synthesized a new phosmidosine analog having an *N*-acylsulfamoyl linkage. An L-alanine-substituted derivative **10** and its derivative **14** were also synthesized in a similar manner. The biological properties of these new compounds were studied and it was found that 5′-*O*-sulfamoyl-8-oxo-adenosine **14** showed potent activity against human cancer cells. Further studies on the mode of action of these compounds are in progress.

## EXPERIMENTAL

$^1$H and $^{13}$C NMR spectra were obtained at 270 and 68 MHz, respectively. The chemical shifts were measured from DMSO-$d_6$ (2.49 ppm) and 3-(trimethylsilyl)propionic-2,2,3,3-$d_4$ acid sodium salt (TSP-$d_4$) (0 ppm) for $^1$H NMR and from DMSO-$d_6$ (39.7 ppm) for $^{13}$C NMR. Column chromatography was performed with silica gel C-200. Reverse-phase column chromatography was performed by use of 37-55 $\mu$m $C_{18}$ particle. Mass spectra were measured by use of an ESI-mass spectrophotometer. *In vitro* analysis of the antitumor activity in cancer cell lines was carried out by the literature method reported by Carmichael[19] and us.[15] The morphological reversion activity test was conducted according to the literature method.[10] Compound **5** was synthesized according to our previous paper.[15]

*2′,3′-O-Isopropylidene-5′-O-sulfamoyl-8-oxoadenosine (**6**).* Under argon atmosphere, compound **5** (1.51 g, 5 mmol) was coevaporated three times with dry pyridine and dissolved in dry DME (25 ml). To this DME solution was added sodium hydrate (60%, 480 mg, 12 mmol), and the mixture was stirred at 0°C for 30 min. A DME (25 ml) solution of sulfamoyl chloride (1.16 g, 10 mmol) was added to the mixture. After being stirred at room temperature for 10 h, the mixture was quenched by addition of 20 ml of methanol and evaporated under reduced pressure. The residue was purified by silica gel column chromatography ($CHCl_3$:methanol = 95:5, v/v) to give compound **6** (1.79 g, 89%): $^1$H NMR (DMSO-$d_6$) $\delta$ 1.31 (3H, s), 1.51 (3H, s), 4.05–4.32 (3H, m), 4.98 (1H, d, $J_{2',3'}$ = 6.3 Hz), 5.39 (1H, d, $J_{2',3'}$ = 6.3 Hz), 5.93 (1H, s), 7.15 (2H, bs), 7.54 (2H, bs), 8.17 (1H, s), 10.94 (1H, bs); $^{13}$C NMR

(DMSO-$d_6$)$\delta$ 25.1, 26.9, 68.3, 79.2, 81.6, 82.4, 84.3, 86.2, 103.5, 113.1, 146.0, 147.2, 151.0, 151.1. ESI-mass $m/z$ cald for $C_{13}H_{19}N_6O_7S$ 403.1036; observed [M + H] 403.1042.

*2′,3′-O-Isopropylidene-5′-O-[N-(boc-L-prolyl)sulfamoyl]-8-oxoadenosine* (**9**). Under argon atmosphere, compound **6** (805 mg, 2 mmol) was coevaporated three times with dry pyridine, and *N*-Boc-L-proline *N*-hydroxysuccinimide ester (750 mg, 2.4 mmol) was added. The mixture was dissolved in dry acetonitrile (20 ml). To this solution, DBU (0.72 ml, 4.8 mmol) was slowly added. After being stirred at room temperature for 4 h, the mixture was diluted by addition of methanol (10 ml) and evaporated under reduced pressure. The residue was purified by silica gel column chromatography ($CHCl_3$:methanol = 95:5, v/v) to give compound **9** (983 mg, 82%): $^1$H NMR (DMSO-$d_6$) $\delta$ 1.25 (9H, s), 1.29 (3H, s), 1.34 (3H, s), 1.60–2.05 (3H, m), 3.07–3.52 (4H, m), 3.79–3.90 (2H, m), 4.00–4.10 (3H, m), 4.14–4.23 (2H, m), 4.87–4.93 (1H, m), 5.41 (1H, m), 5.86 (1H, s$J_{1',2'}$ = 5.6 Hz), 6.95 (2H, bs), 7.99 (1H, s), 11.26 (1H, bs). ESI-mass $m/z$ calcd for $C_{23}H_{34}N_7O_{10}S$ 600.2088; observed [M + H] 600.2080.

*5′-O-[N-(L-prolyl)sulfamoyl]-8-oxoadenosine* (**10**). Compound **9** (599 mg, 1 mmol) was dissolved in 80% formic acid (10 ml). After being stirred at room temperature for 12 h, the mixture was diluted by addition of water and extracted with ethyl acetate. The aqueous layer was collected in a flask and evaporated under reduced pressure. The residue was purified by reverse-phase column chromatography ($H_2O$:methanol = 100:0–97:3, v/v) to give compound **10** as an amorphous white solid (271 mg, 59%): $^1$H NMR ($D_2O$) $\delta$ 1.98–2.15 (4H, m), 2.40–2.55 (1H, m), 3.34–3.53 (2H, m), 4.31 (1H, m), 4.37–4.52 (2H, m), 4.83–4.90 (1H, m), 5.01–5.06 (1H, m), 6.09 (1H, s), 8.45 (1H, s). ESI-mass $m/z$ calcd for $C_{15}H_{22}N_7O_8S$ 460.1251; observed [M + H] 460.1245.

*2′,3′-O-Isopropylidene-5′-O-[N-(boc-L-alanyl)sulfamoyl]-8-oxoadenosine* (**12**). A reaction similar to that described for the synthesis of **9** by use of **6** (805 mg, 2 mmol) and *N*-Boc-L-alanine *N*-hydroxysuccinimide ester **11** (687 mg, 2.4 mmol) gave compound **12** (1.02 g, 89%): $^1$H NMR (DMSO-$d_6$) $\delta$ 1.10 (9H, s), 1.16 (3H, d, $J$ = 5.9 Hz), 1.28 (3H, s), 1.38 (3H, s), 3.81–3.89 (2H, m), 4.00–4.11 (3H, m), 4.16–4.21 (1H, m), 4.85–5.01 (2H, m), 5.90 (1H, s), 7.00 (2H, bs), 7.86 (1H, s), 11.23 (1H, bs). ESI-mass $m/z$ calcd for $C_{21}H_{32}N_7O_{10}S$ 574.1931; observed [M + H] 574.1944.

*5′-O-[N-(L-alanyl)sulfamoyl]-8-oxoadenosine* (**13**). A reaction similar to that described for the synthesis of **10** by use of **12** (217 mg, 0.5 mmol) gave compound **13** (134 mg, 62%): $^1$H NMR ($D_2O$) $\delta$ 1.02 (3H, d, $J$ = 5.9 Hz), 3.79–3.86 (1H, m), 4.17–4.22 (1H, m), 4.37–4.43 (1H, m), 4.50–4.60 (1H, m), 4.75–4.90 (2H, m), 5.98 (1H, s), 8.33 (1H, s); ESI-mass $m/z$ calcd for $C_{13}H_{20}N_7O_8S$ 434.1094; observed [M + H] 434.1082.

*5′-O-Sulfamoyl-8-oxoadenosine* (**14**). Compound **6** (599 mg, 1 mmol) was dissolved in 80% formic acid (10 ml). After being stirred at room temperature for 12 h, the mixture was diluted by addition of water and extracted with ethyl acetate. The aqueous layer was collected in a flask and evaporated under reduced pressure. The residue was purified by reverse-phase column chromatography ($H_2O$:methanol = 100: 0–97:3, v/v) to give compound **14** as an amorphous white solid (271 mg, 62%): $^1H$ NMR (DMSO-$d_6$) $\delta$ 3.98–4.11 (2H, m), 4.22–4.37 (2H, m), 4.80–4.89 (1H, m), 5.28 (1H, d, $J_{2',3'} = 5.1$ Hz), 5.40 (1H, d, $J_{2',3'} = 5.1$ Hz), 5.69 (1H, d, $J_{1',2'} = 4.6$ Hz), 6.59 (2H, bs), 7.50 (2H, bs), 8.02 (1H, s), 10.50 (1H, bs). ESI-mass $m/z$ calcd for $C_{10}H_{15}N_6O_7S$ 363.0723; observed [M + H] 363.0715.

## REFERENCES


1. Koroniak, L.; Ciustea, M.; Gutierrez, J.A.; Richards, G.J. Synthesis and characterization of an *N*-acylsulfonamide inhibitor of human asparagine synthetase. Organic Letters **2003**, 5, 2033.
2. Heacock, D.; Forsyth, C.J.; Shiba, K.; Musier-Forsyth, K. Synthesis and aminoacyl-tRNA synthetase inhibitory activity of prolyl adenylate analogs. Bioorganic & Medicinal Chemistry **1996**, 24, 273.
3. Yu, X. Y.; Hill, J. M.; Yu, G.; Wang, W.; Kluge, A. F.; Wendler, P.; Gallant, P. Synthesis and structure-activity relationships of a series of novel thiazoles as inhibitors of aminoacyl-tRNA synthetases. Bioorganic & Medicinal Chemistry Letters **1999**, 9, 375.
4. Florini, J.R.; Bird, H.H.; Bell, P.H. Inhibition of protein synthesis *in vitro* and *in vivo* by nucleocidin, an antitrypanosomal antibiotic. Journal of Biological Chemistry **1966**, 241, 1091.
5. Jenkins, I.D.; Verheyden, J.P.H.; Moffatt, J.G. 4′-substituted nucleosides 2. Synthesis of the nucleoside antibiotic nucleocidin. Journal of the American Chemical Society **1976**, 98, 3346.
6. Isono, K.; Uramoto, M.; Kusakabe, N.; Miyata, T.; Koyama, M.; Ubukata, M.; Sethi, K.; McCloskey, J.M. Ascamycin and dealanylascamycin, nucleoside antibiotics from *Streptomyces* sp. Journal of Antibiotics **1984**, 37, 670.
7. Ubukata, M.; Osada, H.; Magae, J.; Isono, K. Synthesis Biological activity of aminoacyl analogs of ascamycin. Agricultural & Biological Chemistry **1988**, 52, 1117.
8. Sudo, T.; Shinohara, K.; Dohmae, N.; Takio, K.; Usami, R.; Horikoshi, K.; Osada, H. Isolation and characterization of the gene encoding an aminopeptidase involved in the selective toxicity of ascamyscin toward *Xanthomonas campestris pv. Citri*. Biochemical Journal **1996**, 319, 99.
9. Uramoto, M.; Kim, C.J.; Shin-ya, K.; Kusakabe, H.; Isono, K.; Philips, D.R.; McCloskey, J.A. Isolation and characterization of phosmidosine, a new antifungal nucleotide antibiotic. Journal of Antibiotics **1991**, 44, 375.
10. Matsuura, N.; Onose, R.; Osada, H. Morphology reversion activity of phosmidosine and phosmidosine B, a newly isolated derivative, on src transformed NRK cells. Journal of Antibiotics **1996**, 49, 361.
11. Kakeya, H.; Onose, R.; Liu, P.C.C.; Onozawa, C.; Matsumura, F.; Osada, H. Inhibition of cyclin D1 expression and phosphorylation of retinoblastoma protein by phosmidosine, a nucleotide antibiotic. Cancer Research **1998**, 58, 704.
12. Phillips, D.R.; Uramoto, M.; Isono, K.; McCloskey, J.A. Structure of the antifungal nucleotide antibiotic phosmidosine. Journal of Organic Chemistry **1993**, 58, 854.
13. Moriguchi, T.; Asai, N.; Wada, T.; Seio, K.; Sasaki, T.; Sekine, M. Synthesis and antitumor activities of phosmidosine A and its *N*-acetylated derivative. Tetrahedron Letters **2000**, 41, 5881.
14. Moriguchi, T.; Asai, N.; Okada, K.; Seio, K.; Sasaki, T.; Sekine, M. First synthesis and anticancer activity of phosmidosine and its related compounds. Journal of Organic Chemistry **2002**, 67, 3290.
15. Sekine, M.; Okada, K.; Seio, K.; Kakeya, H.; Osada, H.; Obata, T.; Sasaki, T. Synthesis of chemically stabilized phosmidosine analogues and the structure-activity relationship of phosmidosine. Journal of Organic Chemistry **2003**, 69, 314.

16. Sekine, M.; Okada, K.; Seio, K.; Kakeya, H.; Osada, H.; Sasaki, T. Structure-activity relationship of phosmidosine: Importance of the 7, 8-dihydro-8-oxoadenosine residue for antitumor activity. Bioorganic & Medicinal Chemistry 2004, 12, 5193.
17. Sekine, M.; Okada, K.; Seio, K.; Sasaki, T.; Kakeya, H.; Osada, H. Synthesis of a biotin-conjugate of phosmidosine *O*-ethyl ester as a G1 arrest antitumor drug. Bioorganic & Medicinal Chemistry 2004 12, 6343.
18. Appel, R.; Berger, G. Hydrazinesulfonic acid amide. I. hydrazodisulfamide. Chemische Berichte 1958, 91, 1339.
19. Carmichael, D.W.G.; Gazar, A.F.; Minna, J.D.; Mitchell, J.B. Evaluation of a tetrazolium-based semi-automated colorimetric assay: Assessment of chemosensitivity testing. Cancer Research 1987, 47, 936.

online data

# Epolactaene binds human Hsp60 Cys$^{442}$ resulting in the inhibition of chaperone activity

Yoko NAGUMO*, Hideaki KAKEYA*, Mitsuru SHOJI†, Yujiro HAYASHI†, Naoshi DOHMAE‡ and Hiroyuki OSADA*[1]

*Antibiotics Laboratory, Discovery Research Institute RIKEN, 2-1 Hirosawa, Wako, Saitama 351-0198, Japan, †Department of Industrial Chemistry, Faculty of Engineering, Tokyo University of Science, Kagura-zaka, Shinjuku-ku, Tokyo 162-8601, Japan, and ‡Biomolecular Characterization Team, RIKEN Discovery Research Institute, 2-1 Hirosawa, Wako, Saitama 351-0198, Japan

Epolactaene is a microbial metabolite isolated from *Penicillium* sp., from which we synthesized its derivative ETB (epolactaene tertiary butyl ester). In the present paper, we report on the identification of the binding proteins of epolactaene/ETB, and the results of our investigation into its inhibitory mechanism. Using biotin-labelled derivatives of epolactaene/ETB, human Hsp (heat-shock protein) 60 was identified as a binding protein of epolactaene/ETB *in vitro* as well as *in situ*. In addition, we found that Hsp60 pre-incubated with epolactaene/ETB lost its chaperone activity. The *in vitro* binding study showed that biotin-conjugated epolactaene/ETB covalently binds to Hsp60. In order to investigate the binding site, binding experiments with alanine mutants of Hsp60 cysteine residues were conducted. As a result, it was suggested that Cys$^{442}$ is responsible for the covalent binding with biotin-conjugated epolactaene/ETB. Furthermore, the replacement of Hsp60 Cys$^{442}$ with an alanine residue renders the chaperone activity resistant to ETB inhibition, while the alanine replacement of other cysteine residues do not. These results indicate that this cysteine residue is alkylated by ETB, leading to Hsp60 inactivation.

Key words: chaperone activity, citrate synthase, covalent binding, epolactaene, heat-shock protein 60 (Hsp60), malate dehydrogenase.

## INTRODUCTION

Epolactaene is a microbial metabolite isolated from the fungal strain *Penicillium* sp. BM 1689-P [1]. It was originally shown to be effective in promoting neurite outgrowth and arresting the cell cycle at the $G_0/G_1$ phase in a human neuroblastoma cell line, SH-SY5Y [2]. A study about epolactaene on DNA polymerase inhibition has been conducted [3,4]; however, there is no direct evidence that epolactaene interacts with those proteins in the cell. Therefore we began to study epolactaene-binding proteins in order to investigate how epolactaene affects cellular proteins and their functions.

The Hsp (heat-shock protein) 60 family is known to assist correct protein folding [5]; in addition, mammalian Hsp60 seems to have several functions in the cell, including apoptosis [6–9], an immunoregulatory function [10,11] and cell spreading [12]. Despite the importance of this molecule, little research has been conducted into mammalian Hsp60 compared with members of the prokaryotic Hsp60 family, such as GroEL. Although there is approx. 50% sequence identity between mammalian Hsp60 and GroEL [13], they are not completely similar in structure. GroEL works only in the form of a 14-mer, double ring structure [14,15]. In contrast, human mitochondrial Hsp60 has been reported to be able to assist in protein folding in the form of a 7-mer, single ring structure [16,17]. It is also notable that mitochondrial Hsp60 is functionally active only with co-chaperone Hsp10, whereas GroEL can assist protein folding with either GroES or Hsp10 [14]. Further studies are needed to gain a detailed understanding of the molecular chaperone mechanism and functions of human Hsp60. In the present paper, we demonstrate that epolactaene and its derivative ETB (epolactaene tertiary butyl ester) bind to Hsp60 and inhibit its chaperone activity.

## EXPERIMENTAL

### Reagents

Monoclonal anti-Hsp60 antibody was purchased from BD Biosciences (San Jose, CA, U.S.A.). ETB was synthesized as reported in our synthetic study of epolactaene [18]. Biotin-conjugated ETB (bio–ETB) was synthesized by a coupling reaction using an activated biotin reagent [19]. The structures of ETB, its analogue and bio–ETB were determined by NMR analysis and MS.

### Cell lines and culture

Human neuroblastoma SH-SY5Y cells and human cervix carcinoma HeLa cells were cultured in Dulbecco's modified Eagle's medium (Sigma, St. Louis, MO, U.S.A.), supplemented with 10% (v/v) heat-inactivated foetal calf serum (JRH Bioscience, Lenexa, KS, U.S.A.), 50 units/ml penicillin, 50 $\mu$g/ml streptomycin (Sigma) and 1 mM sodium pyruvate (Gibco, Invitrogen Corporation, Carlsbad, CA, U.S.A.) in 5% $CO_2$ at 37 °C. T-lymphoma Jurkat cells were maintained in RPMI 1640 medium (Sigma) supplemented with 10% (v/v) heat-inactivated foetal calf serum, 50 units/ml penicillin and 50 $\mu$g/ml streptomycin.

### Detection of epolactaene/ETB-binding proteins

The general procedure used to prepare the cell lysates for the detection of binding proteins has been described previously [20,21]. The lysates were incubated with or without ETB as a competitor, followed by the treatment with bio–ETB. After incubation for 1 h at 4 °C, proteins associated with bio–ETB were precipitated with streptavidin–agarose (Oncogene, San Diego, CA, U.S.A.). The bound proteins were eluted with SDS/PAGE loading buffer,

Abbreviations used: CS, citrate synthase; ETB, epolactaene tertiary butyl ester; bio–ETB, biotin-conjugated ETB; i-ETB, inactive ETB analogue; bio–i-ETB, biotin-conjugated i-ETB; HRP, horseradish peroxidase; Hsp, heat-shock protein; LC, liquid chromatography; MDH, malate dehydrogenase; NEM, *N*-ethylmaleimide; SAR, structure–activity relationship.

[1] To whom correspondence should be addressed (email hisyo@riken.jp).

separated by SDS/7.5 % PAGE, and visualized by silver staining. For immunological analysis, the separated proteins were subjected to Western blot analysis.

For the *in situ* binding assay, Jurkat cells were treated with several concentrations of biotin-conjugated derivatives for 2 h. The cells were collected in lysis buffer (10 mM Tris/HCl, pH 7.6, 1 % Nonidet P40, 0.1 % sodium deoxycholate, 0.1 % SDS and 0.15 M NaCl) containing Complete protease inhibitors (Roche, Mannheim, Germany), and the supernatants were then prepared by centrifugation at 800 *g* for 5 min, followed by centrifugation at 20000 *g* for 15 min at 4 °C. Immobilized streptavidin magnetic beads (Promega, Madison, WI, U.S.A.) were added to the lysates, and the mixtures were incubated for 3 h at 4 °C. The bound proteins were washed and eluted by SDS/PAGE loading buffer with boiling. The separated proteins were transferred and analysed by immunoblotting with the anti-Hsp60 antibody.

### Construction of human mitochondrial Hsp60–$His_6$ expression vector

A full-length cDNA encoding the precursor form of human mitochondrial Hsp60 [22] obtained from a Jurkat cDNA library (kindly provided by Dr S. Simizu of RIKEN) was modified so as to provide a translational start codon (AUG) at 5′ to $Ala^{27}$, the first amino acid of the mature protein, as described previously [23]. To this was also added a C-terminal extension of eight amino acids (LEHHHHHH), the last six being a hexahistidine tag. Two PCR primers were employed: primer 1 (5′-GCCATATGGCCAAAGATGTAAAATTTGGTG-3′) introduced an NdeI site (underlined) at the initiator methionine, while primer 2 (5′-CGCCTCGAGGAACATGCCACCTCCCATAC-3′) introduced an XhoI site (underlined) upstream of the stop codon. The PCR product was cut with NdeI and XhoI, and was ligated into the expression vector pET-21b(+) (Novagen, Darmstadt, Germany) digested with the same enzymes. The DNA sequence of this novel fusion protein was confirmed, and it will be referred to throughout the present paper as Hsp60–$His_6$.

### Purification of recombinant mitochondrial Hsp60–$His_6$

*Escherichia coli* BL21(DE3) pLysS, transformed with the vector, was grown in LB (Luria–Bertani) medium with 100 $\mu$g/ml ampicillin at 28 °C. At a $D_{600}$ of 0.4, IPTG (isopropyl $\beta$-D-thiogalactoside) was added to 1 mM, and the cells were shaken for an additional 10 h. A soluble cell extract was prepared, and the mitochondrial Hsp60–$His_6$ was purified with $Ni^{2+}$-nitrilotriacetate–agarose (Qiagen, Hilden, Germany) and desalted with PBS by dialysis.

### Mutagenesis and mutant expression

The mutageneses of $Cys^{237}$ to Ala (for Hsp60-1), $Cys^{442}$ to Ala (Hsp60-2) and $Cys^{447}$ to Ala (Hsp60-3) were performed according to the method described previously [24], using a mutagenic primer for Hsp60-1 (5′-CAAAAGGTCAGAAAGCTGAGTTCCAGGATG-3′), Hsp60-2 (5′-GTTTTGGGAGGGGGCGCCGCCCTCCTTCG-3′) or Hsp60-3 (5′-GTGCCCTCCTGCGCGCCATTCCAGCCTTG-3′). The entire sequences of Hsp60-1, 2 and 3 were analysed to ensure that only the desired mutation had been introduced. The mutant Hsp60–$His_6$ proteins were prepared as described above.

### Chaperone activity of Hsp60

The chaperone activity of human Hsp60 (Stressgen Biotechnologies Corp., Victoria, BC, Canada) was measured using porcine heart CS (citrate synthase) (Sigma) [25] and porcine heart malate dehydrogenase (MDH) (Nacalai Tesque, Kyoto, Japan) [16], as described previously. Briefly, CS was denatured at a concentration of 15 $\mu$M in a buffer containing 6 M guanidinium chloride, 100 mM Tris/HCl, pH 8, and 20 mM dithioerythritol. Reactivation was initiated by diluting the denatured CS 100-fold into a buffer containing 100 mM Tris/HCl, pH 7.6, 10 mM $MgCl_2$, 10 mM KCl and 2 mM ATP at 20 or 35 °C with or without chaperones. Detailed information on the individual experiments are given in the legend to Figure 4. Human Hsp10 was also cloned and prepared as described previously [26]. To reconstitute the chaperone complex, Hsp60 and Hsp10 were mixed and incubated in reconstitution buffer (50 mM Tris/HCl, pH 7.6, 300 mM NaCl, 20 mM KCl, 20 mM magnesium acetate and 4 mM ATP) for 90 min at 30 °C.

For the MDH refolding assays, folding reactions were performed in 0.1 M Tris/HCl, pH 7.6, 7 mM KCl, 7 mM $MgCl_2$ and 10 mM dithiothreitol (buffer A). Porcine MDH (1 $\mu$M) was denatured in 10 mM HCl at room temperature (25 °C) for 2 h and diluted 10-fold into buffer A containing chaperones (2.1 $\mu$M Hsp60 and 4.2 $\mu$M Hsp10) pre-incubated in a reconstitution buffer. After incubation at 27 °C for 5 min, folding was initiated by the addition of 2 mM ATP. For the measurement of the ETB dose–response on the inhibition of Hsp60 mutant chaperone activities, wild-type and mutant Hsp60–$His_6$ proteins were used.

### Hsp60 binding assay

For the *in vitro* binding assay, recombinant Hsp60–$His_6$ was pretreated in the presence or the absence of 10 $\mu$M NEM (*N*-ethylmaleimide) as the competitor, and then treated with bio–ETB at 4 °C. The protein samples were separated by SDS/PAGE and detected by Western blotting using avidin-conjugated HRP (horseradish peroxidase) (Pierce, Rockford, IL, U.S.A.).

Proteins were purchased from Stressgen for the binding experiment of bio–ETB with human Hsp60, Hsp70 and Hsp90. A mixture of 0.7 $\mu$M Hsp60, Hsp70 and Hsp90 was incubated with 0.35 $\mu$M bio–ETB for 1 h at 4 °C, and subjected to SDS/PAGE and Western blotting analysis.

## RESULTS

### Epolactaene derivatives for the screening of binding proteins

To investigate how epolactaene affects cellular proteins, we began to search for epolactaene-binding proteins in a cell lysate. During the SAR (structure–activity relationship) study for epolactaene [19], we synthesized a potent derivative, ETB, and an inactive derivative, i-ETB (Figure 1). We found that ETB is as effective as epolactaene in inhibiting the growth of several human cancer cell lines. Because of the ease of synthetic preparation, we used ETB instead of epolactaene in further studies.

On the basis of observations from the SAR studies, we also prepared bio–ETB and a biotin-conjugated inactive ETB (bio–i-ETB). ETB and i-ETB are conjugated with a biotin moiety at the ester position with an alkyl chain linker (Figure 1). Bio–ETB was found to retain the ability to inhibit growth on the SH-SY5Y and Jurkat cells, whereas bio–i-ETB was as inactive as i-ETB [19].

### Identification of Hsp60 as an epolactaene/ETB-binding protein *in vitro* and *in situ*

With the biotin-conjugated probes in hand, we searched for the epolactaene/ETB-binding proteins. An SH-SY5Y cell extract was incubated with several concentrations of bio–ETB, and the bound

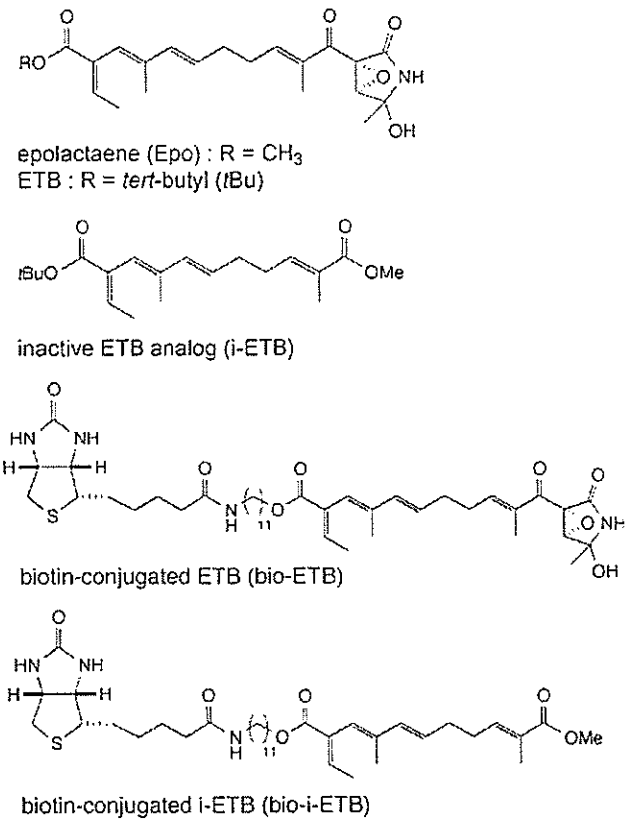


**Figure 1 Chemical structures of epolactaene, ETB, i-ETB and biotin conjugates**

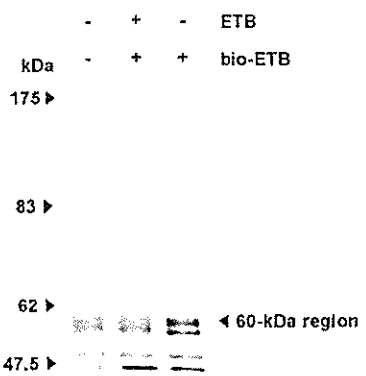


**Figure 2 Screening of ETB-binding proteins**

A SH-SY5Y cell lysate was pre-incubated with 70 $\mu$M ETB as a competitor, followed by treatment with 4 $\mu$M biotinylated ETB. The bound proteins were precipitated with streptavidin beads. The proteins eluted were analysed by SDS/7.5% PAGE, followed by silver staining. Molecular masses are indicated in kDa to the left of the gel.

proteins were precipitated with streptavidin beads and detected by silver staining. To minimize false positives, we used ETB as a competitor. There was a band at approx. 60 kDa, which disappeared when ETB was added as a competitor (Figure 2). Next, a large amount of eluted proteins was analysed by Coomassie Brilliant Blue staining to apply liquid chromatography (LC)–MS analysis. The 60 kDa regions were excised and digested with lysyl endopeptidase, and then the resulting peptide mixture was

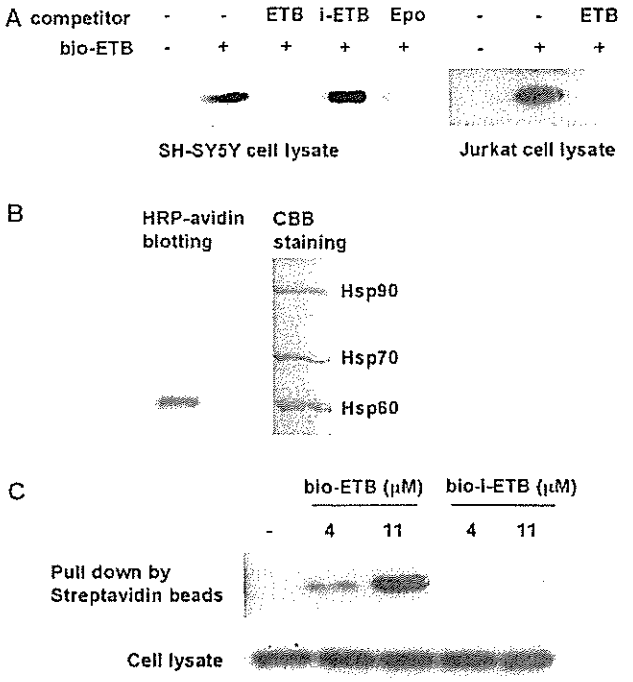


**Figure 3 Identification of Hsp60 as the epolactaene/ETB-binding protein**

(**A**) Immunoblot analysis of the 60 kDa protein bound to epolactaene/ETB. SH-SY5Y cell lysates were pre-incubated with 130 $\mu$M of each competitor, and the Jurkat cell lysates were pre-treated with or without 70 $\mu$M ETB, followed by 13 $\mu$M bio–ETB. The bound proteins were precipitated with streptavidin beads. These proteins were analysed by immunoblotting with the anti-Hsp60 antibody. (**B**) Binding experiment of bio–ETB with Hsp60, Hsp70 and Hsp90 *in vitro*. An equimolar mixture of human Hsp60, Hsp70 and Hsp90 was incubated with bio–ETB for 1 h at 4 °C. The proteins were separated by SDS/PAGE and analysed by HRP-conjugated avidin blotting and Coomassie Brilliant Blue (CBB) staining. (**C**) Binding of bio–ETB to Hsp60 *in situ*. Jurkat cells in culture were treated with biotin-conjugated derivatives for 2 h. The cells were collected in a lysis buffer. Immobilized streptavidin was added to the lysates, and the mixtures were incubated for 3 h at 4 °C. The bound proteins (upper panel) and whole lysates (lower panel) were analysed by immunoblotting with the anti-Hsp60 antibody.

subjected to LC–MS and MS/MS analysis. The peptide fragment from the 60 kDa band was assigned to residues 370–387 of human Hsp60 [RIQEIIEQLDVTTSEYEK, $(M + H)^+$ calculated, 2195.4; found, 2195.7]. To confirm Hsp60 as an epolactaene/ETB-binding protein, we analysed the binding protein using an anti-Hsp60 antibody (Figure 3). Western blotting experiments with the anti-Hsp60 antibody showed that Hsp60 bound to epolactaene/ETB specifically, because an excess of epolactaene/ETB blocked this association, but i-ETB did not. This association was also found in the Jurkat cell lysate, as shown in Figure 3(A). In addition, when we treated bio–ETB with an equimolar mixture of human Hsp60, Hsp70 and Hsp90 *in vitro*, Hsp60 was mainly labelled by bio–ETB (Figure 3B).

To examine whether the binding between epolactaene/ETB and Hsp60 can occur in the cells, we analysed this association *in situ* using bio–ETB derivatives. Jurkat cells were cultured with bio–ETB or bio–i-ETB for 2 h. The biotin-containing complexes were then isolated by streptavidin-immobilized beads, and the bound proteins were analysed by immunoblotting. The samples containing bio–ETB reacted with the anti-Hsp60 antibody in a concentration-dependent manner, whereas those containing bio–i-ETB showed no detectable band, demonstrating that Hsp60 bound specifically to bio–ETB (Figure 3C). These data indicate that epolactaene/ETB can bind to Hsp60 in living cells.

### Inhibition by epolactaene/ETB of the chaperone activity of Hsp60

Hsp60 is a molecular chaperone which assists in protein folding. Mammalian Hsp60 was found to have two forms: cytoplasmic precursor Hsp60 and mitochondrial Hsp60. Although the two forms differ in that the former has a signal sequence in the N-terminus of the protein (1–26 amino acid residues), while the latter does not, both proteins exhibit molecular chaperone activity *in vitro* [27]. In the present study, we used recombinant human mitochondrial Hsp60 for the measurement of chaperone activity.

To determine whether epolactaene/ETB affects the chaperone activity of Hsp60, we assessed the effect of epolactaene/ETB binding on the activity of human recombinant Hsp60. CS refolding was analysed under permissive conditions (20 °C), where spontaneous reactivation could occur, or under non-permissive conditions (35 °C), where spontaneous reactivation could not occur. As shown in Figure 4(A), CS refolded to its native state in a chaperonin-independent manner under permissive conditions. ETB did not interfere with this reactivation, even at 7 $\mu$M. In contrast, the spontaneous reactivation of CS was not observed at 35 °C (Figure 4B). When either of the proteins (Hsp10 or Hsp60) was added singly, only marginal reactivation was observed. In the presence of the complete chaperonin system consisting of Hsp60 and Hsp10, a remarkable recovery of active CS was observed. When we pre-treated Hsp60 with ETB (a final concentration of 2 $\mu$M at the refolding step), the reactivation was almost completely blocked. In addition, when extra (the same amount as in the first addition) Hsp60 was added to the reaction mixture which included the ETB-pre-treated Hsp60, the reactivation was recovered, but such recovery did not occur when extra Hsp10 (the same amount as in the first addition) was added (results not shown).

In order to confirm that ETB inhibits the chaperone function of Hsp60, the other substrate, mitochondrial MDH, was used. As shown in Figure 4(C), a substantial reactivation of the denatured enzyme was observed in the presence of Hsp60 and Hsp10, although neither protein could induce reactivation when added singly. Again, when we pre-treated Hsp60 with ETB, the reactivation was blocked. The reactivation was recovered by the addition of extra Hsp60 (the same amount as in the first addition), but not by the addition of extra Hsp10 (the same amount as in the first addition) (results not shown). These results indicate that the interaction between Hsp60 and epolactaene/ETB is sufficient to affect Hsp60 chaperone activity.

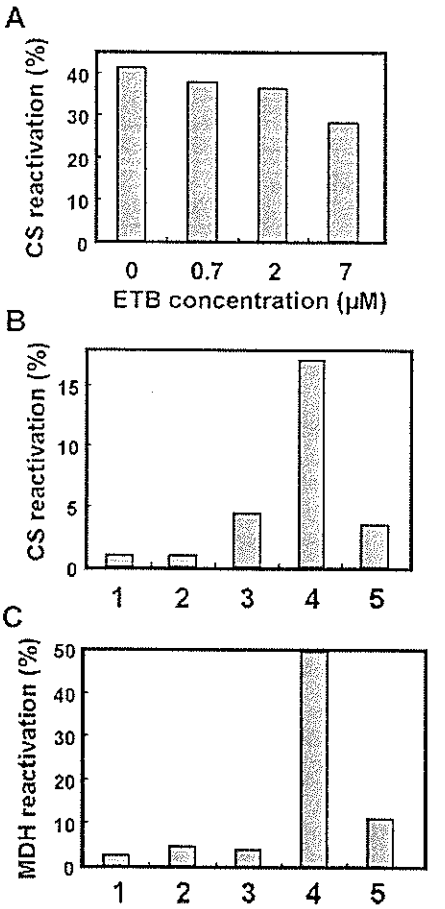


**Figure 4 ETB inhibits the chaperone activity of Hsp60**

The chaperone activity of Hsp60 was analysed under the following conditions. (**A**) Effects of ETB on CS reactivation at permissive conditions. Denatured CS was rapidly diluted to a concentration of 0.15 $\mu$M into a buffer (50 mM Tris/HCl, pH 7.5, 10 mM $MgCl_2$, 10 mM KCl and 15 % glycerol) with various concentrations of ETB at 20 °C. (**B**) Under non-permissive conditions, denatured CS was rapidly diluted to a concentration of 0.15 $\mu$M into a buffer (50 mM Tris/HCl, pH 7.5, 10 mM $MgCl_2$ and 10 mM KCl) containing additives (1.1 $\mu$M Hsp60 or 3.2 $\mu$M Hsp10, or both) at 35 °C. Hsp60 at 14 $\mu$M was pre-incubated with or without 2 molar equivalents of ETB in PBS at 4 °C overnight. ATP (2 mM) was added to the mixture, and after 2 h of incubation, the reactivation of CS was measured. Bar 1, no additives; bar 2, Hsp10 alone; bar 3, Hsp60 alone; bar 4, Hsp60 and Hsp10; bar 5, ETB-pre-treated Hsp60 and Hsp10. (**C**) Effects of ETB using MDH as a substrate. Denatured MDH was rapidly diluted to a concentration of 0.1 $\mu$M into a buffer (0.1 M Tris/HCl, pH 7.6, 7 mM KCl, 7 mM $MgCl_2$ and 10 mM dithiothreitol) containing additives (2.1 $\mu$M Hsp60 or 4.2 $\mu$M Hsp10, or both) at room temperature. Hsp60 was pre-treated with or without ETB, as described in (**B**). ATP (2 mM) was added to the mixture, and, after 30 min, the reactivation of MDH was measured. Bar 1, no additive; bar 2, Hsp10 alone; bar 3, Hsp60 alone; bar 4, Hsp60 and Hsp10; bar 5, ETB-pre-treated Hsp60 and Hsp10.

### $Cys^{442}$ of Hsp60 is responsible for binding with epolactaene/ETB

To determine how epolactaene/ETB modifies the function of Hsp60, we first examined the binding site of Hsp60 with epolactaene/ETB. An *in vitro* binding study (Figure 5A) demonstrated that this binding could last in the SDS/PAGE condition, because it was stained by HRP-conjugated avidin. In addition, this binding was considerably inhibited in the presence of NEM. Because NEM is a Michael acceptor, it was suggested that the covalent binding occurs in a nucleophilic manner. The $\alpha,\beta$-unsaturated ketone, epoxide and hemi-aminal carbon of epolactaene/ETB have an electrophilic character that is potentially reactive with biological nucleophiles, such as the thiols of cysteine residues.

Human Hsp60 has three cysteine residues in the molecule. To confirm that the modification of Hsp60 function occurs as described above, the alanine mutant proteins of each of three cysteine residues (C237A, C442A and C447A) in Hsp60 were prepared in *E. coli* with a C-terminal $His_6$-tag. They were then tested for the ability to bind with bio–ETB. As shown in Figure 5(B), the wild-type Hsp60–$His_6$, C237A and C447A mutants bound with bio–ETB, but C442A lost its binding. These results suggested that $Cys^{442}$ is responsible for covalent binding with bio–ETB.

### Binding of ETB to Hsp60 via $Cys^{442}$ is also important for the inhibition of chaperone activity by ETB

Since the activities of the cysteine mutants of human Hsp60 are not known, we first examined the ability of each mutant to facilitate productive folding. We found that the ability of these altered forms of Hsp60–$His_6$ to productively fold MDH was unimpaired compared with that of the wild-type Hsp60–$His_6$ (Figure 6, open bars).

We next investigated the ETB inhibition effects on both the wild-type and mutant Hsp60–$His_6$ proteins. When each protein was pre-treated with ETB, the chaperone activities of the C237A

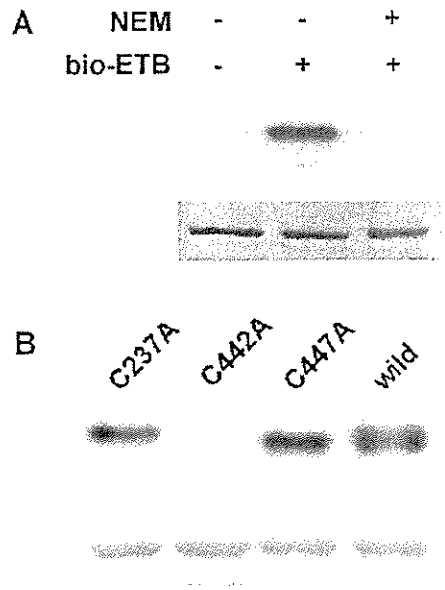


**Figure 5 Cys$^{442}$ of Hsp60 is responsible for binding to epolactaene/ETB**

(A) Competitive effect of NEM on the binding of Hsp60–His$_6$ to bio–ETB. Wild-type Hsp60–His$_6$ (1 $\mu$M) was pre-incubated with or without 10 $\mu$M NEM at 4 °C. After 4 h, 10 $\mu$M bio–ETB was added to the mixture, which was then incubated for an additional 1 h. The proteins were resolved by SDS/7.5 % PAGE and analysed by blotting with HRP-conjugated avidin (upper panel) and CBB staining (lower panel). (B) Binding experiments of the Hsp60 mutants with bio–ETB. The wild-type (wild) and the Hsp60–His$_6$ mutants (14 $\mu$M) were each incubated with 2 molar equivalents of bio–ETB at 4 °C for 12 h. Blotting with HRP-conjugated avidin (upper panel) and Coomassie Brilliant Blue staining (lower panel) were performed as described in (A).

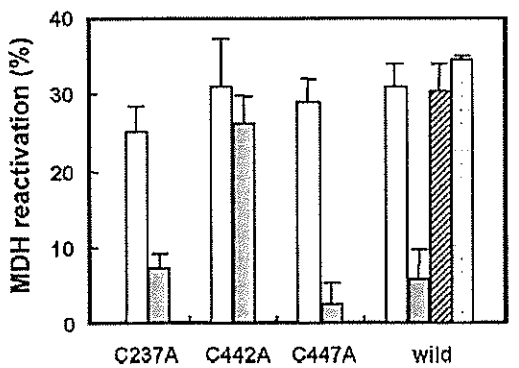


**Figure 6 Inhibition by ETB of Hsp60 mutant chaperone activity on the chaperone-dependent MDH refolding**

Denatured MDH was diluted 10-fold to 0.1 $\mu$M at room temperature by suspending in the buffer containing 2.1 $\mu$M each of Hsp60–His$_6$ mutants and 4.2 $\mu$M Hsp10–His$_6$ or BSA at the same protein concentration. After incubation for 5 min, ATP (2 mM, final concentration) was added to the mixture. At 30 min after the addition of ATP, an aliquot of the mixture was withdrawn, and the recovered MDH activity was measured. The reactivation by each Hsp60–His$_6$ mutant pre-treated with ETB (grey bars; the mutant proteins at 14 $\mu$M in PBS were incubated with 1.8 molar equivalents of ETB at 4 °C for 8 h) or without ETB (open bars) are shown. The reactivation by the wild-type (wild) Hsp60–His$_6$ pre-treated with 1.8 molar equivalents of NEM and 1.8 molar equivalents of mizoribine under the same conditions as ETB are shown by a hatched and a dotted bar respectively. The activity of the same amount of native MDH was taken as 100 %, and then the reactivation (%) by BSA was subtracted as the baseline. The results are the means ± S.D. for three independent experiments.

and C447A mutants, and of the wild-type Hsp60–His$_6$, were considerably inhibited (Figure 6, grey bars). In contrast, the chaperone activity of the C442A mutant was not abolished by ETB pre-treatment. These results indicate that the inhibition of the chaperone activity by ETB pre-treatment is derived mainly from the binding between the ETB and Cys$^{442}$ residue. In addition, these results are in agreement with the binding experiments described above (Figure 5B), which also suggested that ETB inhibits the chaperone activity by binding to Cys$^{442}$ of Hsp60.

Furthermore, we compared the inhibitory effect with NEM and mizoribine, which was reported to interfere with the chaperone activity of Hsp60 and Hsp10 at a higher concentration, 5 mM [28]. Under our experimental conditions, epolactaene/ETB inhibited Hsp60 chaperone activity at a concentration of 2–4 $\mu$M in the refolding reaction mixture. Under the same conditions as epolactaene/ETB (3.8 $\mu$M in the refolding reaction mixture), NEM and mizoribine did not show an inhibitory effect (Figure 6, hatched and dotted bars respectively).

## DISCUSSION

The discovery of the binding proteins of bioactive natural compounds is one strategy for investigating their biological effects. There are many successful precedents, such as the studies on lactacystin [29], fumagillin [30], radicicol [20] and other compounds. With lactacystin, for example, the discovery that the binding target was the 20 S proteasome subunit, and that lactacystin inhibited proteasome activity [29], has promoted the exploration of not only the mode of action of lactacystin, but also the proteasome functions. In this way, the identification of binding proteins furthers biochemical research.

ETB, which is a chemically synthesized derivative of epolactaene, is as effective as epolactaene in inhibiting the growth of several human cancer cell lines [19]. Although several studies on DNA polymerase inhibition have already been conducted [3,4], the $IC_{50}$ values of the DNA polymerase $\alpha$ and $\beta$ inhibition by epolactaene were reported to be 25 and 100 $\mu$M respectively *in vitro*, which are considerably higher than the effective dose on the cell growth inhibition. In the present study, we searched for the binding targets of epolactaene/ETB in order to obtain direct support for the probability that epolactaene interacts with cellular proteins and disturbs its function. There were several specific or non-specific binding proteins *in vitro*, and we successfully identified human Hsp60 using bio–ETB as a bioprobe (Figures 2 and 3). The binding between Hsp60 is specific for epolactaene/ETB because the binding was blocked by the addition of epolactaene/ETB, but not by the addition of inactive analogue i-ETB. Furthermore, the finding that bio–ETB can bind Hsp60 *in situ* indicated that this complex is also formed in living cells (Figure 3C).

To elucidate the details of the interaction between ETB and Hsp60, we prepared Hsp60 mutants. Our analysis of the binding between bio–ETB and the mutant proteins suggested that Cys$^{442}$ of Hsp60 is responsible for the binding (Figure 5B). To determine how this binding affects the Hsp60 chaperone activity, we first analysed the chaperone activity of each cysteine mutant, since the mutants of human Hsp60 have scarcely been explored [16]. We found that the chaperone activity of mutant Hsp60–His$_6$, using MDH as a substrate, was almost the same as that of the wild-type Hsp60–His$_6$ (Figure 6). ETB blocked the chaperone activities of the wild-type protein and of the C237A and C447A mutant proteins, but not that of the C442A mutant (Figure 6), indicating that epolactaene/ETB binding to Cys$^{442}$ disrupts the chaperone activity. Based on sequence alignment and a comparison with the reported GroEL crystal structures [31], Cys$^{442}$ is predicted to lie near the ATP binding site (see Supplemental Figure 1 at http://www.BiochemJ.org/bj/387/bj3870835add.htm), although none of the three cysteine residues in Hsp60 is conserved in GroEL. The ATP pocket is suggested to be important not only for ATPase activity, but also for oligomerization [14,32]. Therefore interaction with

ETB may disturb the nucleotide pocket and result in the loss of ATPase activity or the destabilization of oligomeric structures, or both, although it is difficult to determine which is responsible for the inhibition.

To date, there are scarcely any natural compounds known which bind and inhibit mammalian Hsp60 chaperone activity. The 60 kDa chaperones constitute a family of proteins that play an important role in the folding of nascent, translocated and stress-denatured proteins [5]. In addition, mammalian Hsp60 has been reported to have several functions in the cell [6–12]. Using mizoribine, which inhibits the chaperone activity of mammalian Hsp60/Hsp10 at 5 mM [28], the association of Hsp60 with integrin $\alpha_3\beta_1$ was investigated [12]. Hsp60-binding compounds would be very useful for studying mammalian Hsp60 functions. In the present study, we discovered that bio–ETB covalently binds to $Cys^{442}$ of Hsp60 and inhibits its chaperone activity. As far as we know, this is the first example of human Hsp60 covalently modified by a natural compound in a site-specific way.

In conclusion, we have demonstrated that epolactaene/ETB binds human Hsp60 *in vitro* and *in situ*, and that epolactaene/ETB inhibited the chaperone activity of human Hsp60. Furthermore, we have revealed that $Cys^{442}$ of Hsp60 is responsible for the covalent binding of epolactaene/ETB, and have shown the resistance of the C442A mutant to ETB inhibition, suggesting this binding resulted in the inhibition of the chaperone activity. These observations of how epolactaene/ETB inhibits the chaperone activity will be helpful for gaining an understanding of the human Hsp60 multifunctions and the mechanisms of molecular chaperones.

We are grateful to K. Ishida for his helpful comments. This work was supported in part by a Grant-in-Aid from the Ministry of Education, Culture, Sports, Science and Technology of Japan, by Grant-in-Aid for Cancer Research from the Ministry of Health, Labour, and Welfare of Japan, by the Chemical Biology project (RIKEN), and by funding from the Special Postdoctoral Researchers Program (to Y. N.).

## REFERENCES

1 Kakeya, H., Takahashi, I., Okada, G., Isono, K. and Osada, H. (1995) Epolactaene, a novel neuritogenic compound in human neuroblastoma cells, produced by a marine fungus. J. Antibiot. **48**, 733–735
2 Kakeya, H., Onozawa, C., Sato, M., Arai, K. and Osada, H. (1997) Neuritogenic effect of epolactaene derivatives on human neuroblastoma cells which lack high-affinity nerve growth factor receptors. J. Med. Chem. **40**, 391–394
3 Nakai, J., Kawada, K., Nagata, S., Kuramochi, K., Uchiro, H., Kobayashi, S. and Ikekita, M. (2002) A novel lipid compound, epolactaene, induces apoptosis: its action is modulated by its side chain structure. Biochim. Biophys. Acta **1581**, 1–10
4 Mizushina, Y., Kobayashi, S., Kuramochi, K., Nagata, S., Sugawara, F. and Sakaguchi, K. (2000) Epolactaene, a novel neuritogenic compound in human neuroblastoma cells, selectively inhibits the activities of mammalian DNA polymerases and human DNA topoisomerase II. Biochem. Biophys. Res. Commun. **273**, 784–788
5 Thirumalai, D. and Lorimer, G. H. (2001) Chaperonin-mediated protein folding. Annu. Rev. Biophys. Biomol. Struct. **30**, 245–269
6 Kirchhoff, S. R., Gupta, S. and Knowlton, A. A. (2002) Cytosolic heat shock protein 60, apoptosis, and myocardial injury. Circulation **105**, 2899–2904
7 Shan, Y. X., Liu, T. J., Su, H. F., Samsamshariat, A., Mestril, R. and Wang, P. H. (2003) Hsp10 and Hsp60 modulate Bcl-2 family and mitochondria apoptosis signaling induced by doxorubicin in cardiac muscle cells. J. Mol. Cell. Cardiol. **35**, 1135–1143
8 Samali, A., Cai, J., Zhivotovsky, B., Jones, D. P. and Orrenius, S. (1999) Presence of a pre-apoptotic complex of pro-caspase-3, Hsp60 and Hsp10 in the mitochondrial fraction of Jurkat cells. EMBO J. **18**, 2040–2048
9 Xanthoudakis, S., Roy, S., Rasper, D., Hennessey, T., Aubin, Y., Cassady, R., Tawa, P., Ruel, R., Rosen, A. and Nicholson, D. W. (1999) Hsp60 accelerates the maturation of pro-caspase-3 by upstream activator proteases during apoptosis. EMBO J. **18**, 2049–2056
10 Bethke, K., Staib, F., Distler, M., Schmitt, U., Jonuleit, H., Enk, A. H., Galle, P. R. and Heike, M. (2002) Different efficiency of heat shock proteins (HSP) to activate human monocytes and dendritic cells: superiority of HSP60. J. Immunol. **169**, 6141–6148
11 Kol, A., Lichtman, A. H., Finberg, R. W., Libby, P. and Kurt-Jones, E. A. (2000) Cutting edge: heat shock protein (HSP) 60 activates the innate immune response: CD14 is an essential receptor for HSP60 activation of mononuclear cells. J. Immunol. **164**, 13–17
12 Barazi, H. O., Zhou, L., Templeton, N. S., Krutzsch, H. C. and Roberts, D. D. (2002) Identification of heat shock protein 60 as a molecular mediator of $\alpha_3\beta_1$ integrin activation. Cancer Res. **62**, 1541–1548
13 Venner, T. J., Singh, B. and Gupta, R. S. (1990) Nucleotide sequences and novel structural features of human and Chinese hamster hsp60 (chaperonin) gene families. DNA Cell Biol. **9**, 545–552
14 Viitanen, P. V., Lorimer, G., Bergmeier, W., Weiss, C., Kessel, M. and Goloubinoff, P. (1998) Purification of mammalian mitochondrial chaperonin 60 through *in vitro* reconstitution of active oligomers. Methods Enzymol. **290**, 203–217
15 Weissman, J. S., Rye, H. S., Fenton, W. A., Beechem, J. M. and Horwich, A. L. (1996) Characterization of the active intermediate of a GroEL-GroES-mediated protein folding reaction. Cell **84**, 481–490
16 Nielsen, K. L. and Cowan, N. J. (1998) A single ring is sufficient for productive chaperonin-mediated folding *in vivo*. Mol. Cell **2**, 93–99
17 Levy-Rimler, G., Viitanen, P., Weiss, C., Sharkia, R., Greenberg, A., Niv, A., Lustig, A., Delarea, Y. and Azem, A. (2001) The effect of nucleotides and mitochondrial chaperonin 10 on the structure and chaperone activity of mitochondrial chaperonin 60. Eur. J. Biochem. **268**, 3465–3472
18 Hayashi, Y., Kanayama, J., Yamaguchi, J. and Shoji, M. (2002) Diastereoselective total synthesis of both enantiomers of epolactaene. J. Org. Chem. **67**, 9443–9448
19 Nagumo, Y., Kakeya, H., Yamaguchi, J., Uno, T., Shoji, M., Hayashi, Y. and Osada, H. (2004) Structure–activity relationships of epolactaene derivatives: structural requirements for inhibition of Hsp60 chaperone activity. Bioorg. Med. Chem. Lett. **14**, 4425–4429
20 Ki, S. W., Ishigami, K., Kitahara, T., Kasahara, K., Yoshida, M. and Horinouchi, S. (2000) Radicicol binds and inhibits mammalian ATP citrate lyase. J. Biol. Chem. **275**, 39231–39236
21 Miyake, Y., Kakeya, H., Kataoka, T. and Osada, H. (2003) Epoxycyclohexenone inhibits Fas-mediated apoptosis by blocking activation of pro-caspase-8 in the death-inducing signaling complex. J. Biol. Chem. **278**, 11213–11220
22 Jindal, S., Dudani, A. K., Singh, B., Harley, C. B. and Gupta, R. S. (1989) Primary structure of a human mitochondrial protein homologous to the bacterial and plant chaperonins and to the 65-kilodalton mycobacterial antigen. Mol. Cell. Biol. **9**, 2279–2283
23 Viitanen, P. V., Lorimer, G. H., Seetharam, R., Gupta, R. S., Oppenheim, J., Thomas, J. O. and Cowan, N. J. (1992) Mammalian mitochondrial chaperonin 60 functions as a single toroidal ring. J. Biol. Chem. **267**, 695–698
24 Sawano, A. and Miyawaki, A. (2000) Directed evolution of green fluorescent protein by a new versatile PCR strategy for site-directed and semi-random mutagenesis. Nucleic Acids Res. **28**, E78
25 Schmidt, M., Buchner, J., Todd, M. J., Lorimer, G. H. and Viitanen, P. V. (1994) On the role of groES in the chaperonin-assisted folding reaction: three case studies. J. Biol. Chem. **269**, 10304–10311
26 Dickson, R., Larsen, B., Viitanen, P. V., Tormey, M. B., Geske, J., Strange, R. and Bemis, L. T. (1994) Cloning, expression, and purification of a functional nonacetylated mammalian mitochondrial chaperonin 10. J. Biol. Chem. **269**, 26858–26864
27 Itoh, H., Komatsuda, A., Ohtani, H., Wakui, H., Imai, H., Sawada, K., Otaka, M., Ogura, M., Suzuki, A. and Hamada, F. (2002) Mammalian HSP60 is quickly sorted into the mitochondria under conditions of dehydration. Eur. J. Biochem. **269**, 5931–5938
28 Itoh, H., Komatsuda, A., Wakui, H., Miura, A. B. and Tashima, Y. (1999) Mammalian HSP60 is a major target for an immunosuppressant mizoribine. J. Biol. Chem. **274**, 35147–35151
29 Fenteany, G., Standaert, R. F., Lane, W. S., Choi, S., Corey, E. J. and Schreiber, S. L. (1995) Inhibition of proteasome activities and subunit-specific amino-terminal threonine modification by lactacystin. Science **268**, 726–731
30 Sin, N., Meng, L., Wang, M. Q., Wen, J. J., Bornmann, W. G. and Crews, C. M. (1997) The anti-angiogenic agent fumagillin covalently binds and inhibits the methionine aminopeptidase, MetAP-2. Proc. Natl. Acad. Sci. U.S.A. **94**, 6099–6103
31 Xu, Z., Horwich, A. L. and Sigler, P. B. (1997) The crystal structure of the asymmetric GroEL-GroES-(ADP)7 chaperonin complex. Nature (London) **388**, 741–750
32 Bochkareva, E. S., Horovitz, A. and Girshovich, A. S. (1994) Direct demonstration that ATP is in contact with Cys-137 in chaperonin GroEL. J. Biol. Chem. **269**, 44–46

Received 9 August 2004/1 December 2004; accepted 16 December 2004
Published as BJ Immediate Publication 16 December 2004, DOI 10.1042/BJ20041355

# ECH, an Epoxycyclohexenone Derivative That Specifically Inhibits Fas Ligand-Dependent Apoptosis in CTL-Mediated Cytotoxicity[1]

Tomokazu Mitsui,* Yasunobu Miyake,*† Hideaki Kakeya,† Hiroyuki Osada,† and Takao Kataoka[2]*

**CTL eliminate cells infected with intracellular pathogens and tumor cells by two distinct mechanisms mediated by Fas ligand (FasL) and lytic granules that contain perforin and granzymes. In this study we show that an epoxycyclohexenone derivative, (*2R,3R,4S*)-2,3-epoxy-4-hydroxy-5-hydroxymethyl-6-(*1E*)-propenyl-cyclohex-5-en-1-one (ECH) specifically inhibits the FasL-dependent killing pathway in CTL-mediated cytotoxicity. Recently, we have reported that ECH blocks activation of procaspase-8 in the death-inducing signaling complex and thereby prevents apoptosis induced by anti-Fas Ab or soluble FasL. Consistent with this finding, ECH profoundly inhibited Fas-mediated DNA fragmentation and cytolysis of target cells induced by perforin-negative mouse CD4$^+$ CTL and alloantigen-specific mouse CD8$^+$ CTL pretreated with an inhibitor of vacuolar type H$^+$-ATPase concanamycin A that selectively induces inactivation and proteolytic degradation of perforin in lytic granules. However, ECH barely influenced perforin/granzyme-dependent DNA fragmentation and cytolysis of target cells mediated by alloantigen-specific mouse CD8$^+$ CTL. The components of lytic granules and the granule exocytosis pathway upon CD3 stimulation were also insensitive to ECH. In conclusion, our present results demonstrate that ECH is a specific nonpeptide inhibitor of FasL-dependent apoptosis in CTL-mediated cytotoxicity. Therefore, ECH can be used as a bioprobe to evaluate the contributions of two distinct killing pathways in various CTL-target settings.** *The Journal of Immunology,* **2004, 172: 3428–3436.**

Cytotoxic T lymphocytes play a critical role in protection against intracellular pathogens and tumor cells as well as autoimmunity and transplant rejection. To induce apoptosis of target cells, CTL mainly use two distinct pathways that are dependent on Fas ligand (FasL)[3] and lytic granules that contain the pore-forming protein perforin and serine proteases termed granzymes (1, 2). CD8$^+$ CTL eliminate target cells primarily via the perforin-dependent pathway, whereas the FasL-dependent killing pathway is dominantly used by CD4$^+$ CTL (1). The perforin system is essential for the control of viral infection and tumor rejection, and the Fas/FasL system is important for lymphocyte homeostasis (1, 3–5). However, these two killing systems play different regulatory roles in various physiological and pathogenic situations.

CTL harbor lytic granules that store perforin and granzymes under the acidic environment (6). Upon TCR stimulation, CTL rapidly release lytic granules into the interface between CTL-target conjugates (1, 2). Perforin facilitates the translocation of granzymes A and B into the cytosol without pore formation on the plasma membrane (7). Granzymes A and B are major molecules that induce target cell death (1, 2). Granzyme B initiates caspase-dependent apoptosis that requires the release of proapoptotic mitochondrial factors (8–10). By contrast, granzyme A triggers a caspase-independent alternate cell death pathway characterized by ssDNA nicks (11, 12). However, in the granule-mediated killing pathway, granzyme B is critical for rapid induction of DNA fragmentation in target cells (13).

Upon TCR stimulation, FasL is newly synthesized and then transported to the cell surface of CTL (1). In the cytoplasmic region, Fas contains the death domain that is required for interaction with the adaptor protein Fas-associated death domain protein (FADD) (3–5). Membrane-bound FasL triggers Fas oligomerization, which allows the recruitment of FADD to the Fas death domain (3–5). FADD subsequently binds to procaspase-8 via the mutual interaction of their death effector domain, resulting in the formation of death-inducing signaling complex (DISC) (14). In the DISC, procaspase-8 immediately dimerizes and undergoes self-cleavage, generating the active heterotetramer composed of two large subunits and two small subunits (15, 16). Active caspase-8 cleaves downstream substrates such as procaspase-3 or Bid, essential for apoptosis execution (1–5).

Membrane-permeable small compounds are expected to be valuable tools to clarify the molecular basis of complex intracellular signaling pathways and to be potential therapeutic drugs as well. Hence, specific modulators of CTL-mediated cytotoxicity are highly useful. Previously, we reported that vacuolar type H$^+$-ATPase inhibitor concanamycin A (CMA) is a specific inhibitor of the perforin-dependent killing pathway in target cell lysis mediated by CTL and NK cells (17, 18). However, the FasL-dependent killing pathway is totally insensitive to CMA (18). CMA perturbs acidification of lytic granules and raises

*Division of Bioinformatics, Center for Biological Resources and Informatics, Tokyo Institute of Technology, Yokohama, Japan; and †Antibiotics Laboratory, Discovery Research Institute, RIKEN, Saitama, Japan

Received for publication July 28, 2003. Accepted for publication January 7, 2004.

The costs of publication of this article were defrayed in part by the payment of page charges. This article must therefore be hereby marked *advertisement* in accordance with 18 U.S.C. Section 1734 solely to indicate this fact.

[1] This work was supported by a grant-in-aid for scientific research from the Ministry of Education, Culture, Sports, Science, and Technology and research grants from Kato Memorial Bioscience Foundation and Mitsubishi Pharma Research Foundation. Y.M. was partly supported by the Grant of the 21st Century COE Program, Ministry of Education, Culture, Sports, Science and Technology.

[2] Address correspondence and reprint requests to Dr. Takao Kataoka, Division of Bioinformatics, Center for Biological Resources and Informatics, Tokyo Institute of Technology, 4259 Nagatsuta-cho, Midori-ku, Yokohama 226-8501, Japan. E-mail address: tkataoka@bio.titech.ac.jp

[3] Abbreviations used in this paper: FasL, Fas ligand; FADD, Fas-associated death domain protein; DISC, death-inducing signaling complex; CMA, concanamycin A; ECH, (*2R,3R,4S*)-2,3-epoxy-4-hydroxy-5-hydroxymethyl-6-(*1E*)-propenyl-cyclohex-5-en-1-one; FADD, Fas-associated death domain protein; KLH, keyhole limpet hemocyanin; PCA, penicillic acid.



0022-1767/04/$02.00

the internal pH to around neutral (19). Neutralization of acidic pH induces inactivation of perforin in a $Ca^{2+}$-dependent manner and subsequent proteolytic degradation of perforin by serine proteases (17, 20). To date, CMA has been frequently used to evaluate the contribution of the perforin-dependent killing pathway in cell-mediated cytotoxicity.

The early signal transduction of Fas-mediated apoptosis is a complex process regulated by various cellular proteins exerting proapoptotic and antiapoptotic functions. To search for specific modulators of Fas-mediated apoptosis, we have screened natural products, such as microbial metabolites, and identified several modulators that block or enhance the Fas death signals (21–24). It was reported that an epoxycyclohexenone derivative, (*2R,3R,4S*)-2,3-epoxy-4-hydroxy-5-hydroxymethyl-6-(*1E*)-propenyl-cyclohex-5-en-1-one (ECH; see Fig. 1*A*), prevents Fas-mediated apoptosis (25). However, the molecular target of ECH remained to be elucidated. Recently, we have shown that ECH inhibits apoptosis mediated by Fas and TNF receptor 1 through preventing activation of procaspase-8 in the DISC (24). By contrast, death receptor-independent apoptosis induced by chemical drugs and UV irradiation was totally insensitive to ECH (24). In the present report we have studied the inhibitory effects of ECH on two distinct CTL-mediated killing pathways. Our results demonstrate that ECH does not affect the perforin-dependent killing pathway, but selectively inhibits the FasL-dependent killing pathway mediated by Ag-specific CTL.

## Materials and Methods

### *Cells*

The H-$2^d$-specific $CD8^+$ CTL clone OE4 (26) and the keyhole limpet hemocyanin (KLH)-specific H-$2^d$ (I-$E^d$)-restricted $CD4^+$ CTL clone BK-1 (27) were maintained in RPMI 1640 medium (Invitrogen, Carlsbad, CA) supplemented with 10% (v/v) heat-inactivated FCS (JRH Biosciences, Lenexa, KS), 50 μM 2-ME, 5% (v/v) rat spleen cell-conditioned medium (culture supernatant of rat spleen cells stimulated with 5 μg/ml CMA for 24 h), and penicillin-streptomycin-neomycin antibiotic mixture (Invitrogen). OE4 cells were stimulated with mitomycin C-treated spleen cells prepared from BALB/c mice every 2 wk. BK-1 cells were stimulated with 10 μg/ml KLH (Calbiochem, Darmstadt, Germany) in the presence of mitomycin C-treated BALB/c mouse spleen cells every 2 wk. BALB/c mouse-derived B lymphoma (A20, A20.HL, A20.FO) were maintained in RPMI 1640 medium containing 10% (v/v) FCS, 50 μM 2-ME, and penicillin-streptomycin-neomycin antibiotic mixture. A20.HL cells were the BALB/c B lymphoma transfected with L and H chain genes of anti-TNP IgM Ab (28). A20.FO cells were the Fas-negative variant subcloned from the Fas-positive parent cell line A20.2J (18). DBA/2 mouse-derived T lymphoma L5178Y and the Fas-expressing transfectant of L5178Y (L5178Y-Fas) (29) were maintained in RPMI 1640 medium containing 10% (v/v) FCS, 50 μM 2-ME, and penicillin-streptomycin-neomycin antibiotic mixture.

### *Reagents*

ECH was isolated from the culture broth of a producing fungal strain using a bioassay-guided purification procedure (24). CMA was purchased from Wako Pure Chemical Industries (Osaka, Japan). Recombinant human soluble FasL was a gift from Dr. J. Tschopp (Institute of Biochemistry, University of Lausanne, Epalinges, Switzerland) and was used as described previously (30).

### *DNA fragmentation assay*

Target cells were labeled with 37 kBq of [$^3$H]TdR (ICN Biomedicals, Costa Mesa, CA) for 16 h and washed three times before use. The labeled cells ($1 \times 10^5$ cells/ml, 100 μl) were preincubated with the indicated concentrations of ECH for 1 or 2 h, then mixed with 100 μl of CTL in U-bottom, 96-well microtiter plates. The plates were centrifuged ($300 \times g$, 3 min) and then incubated for 4 h. The drug concentration during coculture with CTL was diluted into half the initial drug concentration. At the end of the culture, 10 μl of 2% Triton X-100 was added to each well, and the cells were lysed by pipetting, followed by centrifugation ($600 \times g$, 5 min). One hundred microliters of supernatants were harvested and measured for radioactivity. Specific $^3$H-labeled DNA release (percentage) was calculated using the following formula: (experimental cpm − spontaneous cpm)/(maximum cpm − spontaneous cpm) × 100.

### *$^{51}$Cr release assay*

Target cells were labeled with 1850 kBq of [$^{51}$Cr]sodium chromate (Amersham Biosciences, Piscataway, NJ) in 100 μl of 50% (v/v) FCS for 1 h and washed three times with the medium. The labeled cells ($1 \times 10^5$ cells/ml, 100 μl) were preincubated with indicated concentrations of ECH for 1 h, then mixed with 100 μl of CTL in U-bottom, 96-well microtiter plates. The plates were centrifuged ($300 \times g$, 3 min) and then incubated for 4 h. One hundred microliters of supernatants were harvested and measured for radioactivity. Specific $^{51}$Cr release (percentage) was calculated using the following formula: (experimental cpm − spontaneous cpm)/(maximum cpm − spontaneous cpm) × 100.

### *Analysis of effector/target conjugate formation*

Analysis of conjugate formation was performed as described previously (31). Target cells ($5 \times 10^5$ cells/ml) were treated with or without ECH for 1 h, then stained with 62.5 μg/ml hydroethidine (Polysciences, Warrington, PA) for 30 min on ice. Effector cells ($5 \times 10^5$ cells/ml) were stained with 0.25 μM calcein-AM (Molecular Probes, Eugene, OR) for 30 min on ice. Both types of stained cells ($5 \times 10^5$ cells/ml, 250 μl) were washed twice with the medium, then transferred in a single tube. The cell mixtures were either left untreated or centrifuged ($300 \times g$, 3 min), then incubated at 25°C for 30 min. The cells were resuspended carefully by pipetting and immediately analyzed by FACS.

### *Western blotting*

OE4 cells ($1 \times 10^6$ cells) were washed with PBS and lysed with 1% Triton X-100, 50 mM Tris-HCl (pH 7.4), and protease inhibitor mixture (Complete; Roche, Mannheim, Germany) on ice for 15 min. After centrifugation ($10{,}000 \times g$, 5 min), supernatants were collected. Postnuclear lysates (30 μg/lane) were separated by 10% SDS-PAGE and analyzed by Western blotting using ECL detection reagents (Amersham Biosciences). Anti-mouse perforin Ab P1-8 (32) was provided by Dr. H. Yagita (Juntendo University School of Medicine, Tokyo, Japan).

### *Measurement of granzyme activity*

OE4 cells ($1 \times 10^6$ cells) were washed with PBS and lysed with 0.5% Triton X-100, 10 mM HEPES-NaOH (pH 7.4), 150 mM NaCl, 1 mM $CaCl_2$, and 1 mM $MgCl_2$ on ice for 15 min. After centrifugation ($10{,}000 \times g$, 5 min), supernatants were collected. Postnuclear lysates (5 μg) were incubated with 200 μl of the reaction mixture (200 μM 5,5′-dithio-bis-(2-nitrobenzoic acid) plus either 200 μM CBZ-Gly-Arg-thiobenzylester for the granzyme A substrate or Boc-Ala-Ala-Asp-thiobenzylester for the granzyme B substrate (Enzyme Systems Products, Dublin, CA) in 10 mM HEPES-NaOH (pH 7.4), 150 mM NaCl, 1 mM $CaCl_2$, and 1 mM $MgCl_2$) at room temperature. Absorbance at 415 nm was measured.

### *Analysis of granule exocytosis*

OE4 cells ($1 \times 10^6$ cells/ml, 100 μl) were transferred into 96-well microtiter plates coated with anti-mouse CD3 Ab 145-2C11 (10 μg/ml). After centrifugation ($300 \times g$, 3 min), the cells were incubated for 4 h. Culture supernatants were removed and measured for the activity of granzyme A as described above.

## Results

### *ECH inhibits DNA fragmentation induced by soluble FasL*

B lymphoma A20 cells are sensitive to Fas-mediated apoptosis and exhibited DNA fragmentation characteristic of apoptosis within 4 h upon exposure to cross-linked FasL, whereas Fas-negative A20.FO cells were totally resistant to cross-linked FasL (Fig. 1*B*). ECH inhibited FasL-induced DNA fragmentation in a dose-dependent manner, and complete inhibition was observed when A20 cells were pretreated with 50–100 μM ECH for 1 h (Fig. 1*C*). ECH was only diluted into half of the initial concentration during exposure to FasL, because DNA fragmentation was partially reversed when ECH was removed from A20 cells during the coculture with FasL (Fig. 1*D*). Under these experimental conditions, ECH was not cytotoxic to the cell, as no DNA fragmentation was induced by ECH alone (Fig. 1*D*). Twenty-four-hour incubation of A20 cells with ECH resulted in a marked reduction of live cell-number without an induction of DNA fragmentation (Fig. 1, *E* and

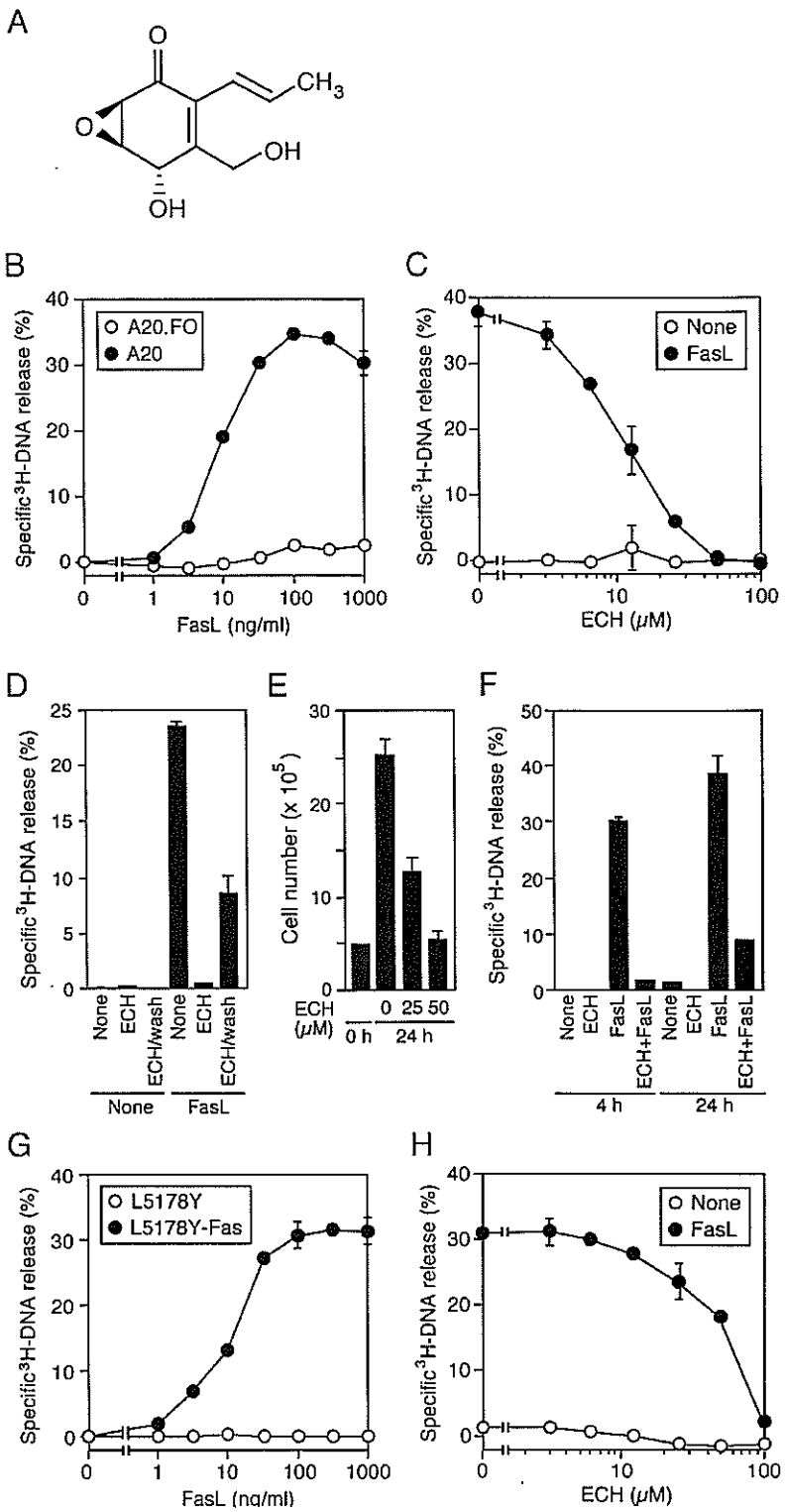


**FIGURE 1.** ECH inhibits DNA fragmentation induced by soluble FasL. *A*, Structure of ECH. *B–D*, [$^3$H]TdR-labeled A20 (●) and A20.FO (○) cells were incubated with various concentrations of cross-linked FasL for 4 h (*B*). [$^3$H]TdR-labeled A20 cells were preincubated with serial dilutions of ECH for 1 h, and then incubated with (●) or without (○) cross-linked FasL (50 ng/ml) for 4 h (*C*). [$^3$H]TdR-labeled A20 cells were preincubated with or without ECH (50 μM) for 1 h and either untreated or washed with the medium to remove ECH, followed by incubation with or without cross-linked FasL (50 ng/ml) for 4 h (*D*). The radioactivity of fragmented DNA was measured. Data points represent the mean ± SD of triplicate cultures. *E*, A20 cells were incubated in the presence of the indicated concentrations of ECH for 24 h. The number of live cells was counted by trypan blue dye exclusion. Data points represent the mean ± SD of triplicate determinations. *F–H*, [$^3$H]TdR-labeled A20 cells were preincubated with or without ECH (50 μM) for 1 h, and then incubated in the presence or the absence of cross-linked FasL (50 ng/ml) for 4 or 24 h (*F*). [$^3$H]TdR-labeled L5178Y-Fas (●) and L5178Y (○) cells were incubated with various concentrations of cross-linked FasL for 4 h (*G*). [$^3$H]TdR-labeled L5178Y-Fas cells were preincubated with serial dilutions of ECH for 2 h and then incubated with (●) or without (○) cross-linked FasL (50 ng/ml) for 4 h (*H*). The radioactivity of fragmented DNA was measured. Data points represent the mean ± SD of triplicate cultures.

*F*). Less than 20% of the total cells were stained with trypan blue when A20 cells were treated with 50 μM ECH for 24 h (data not shown). In addition to A20 cells, the T lymphoma L5178Y cells were used for the second cell line to study the biological activity of ECH. Although L5178Y cells were insensitive to cross-linked FasL, Fas-transfected L5178Y cells (L5178Y-Fas) were highly susceptible to cross-linked FasL (Fig. 1*G*). DNA fragmentation induced by cross-linked FasL was completely inhibited when L5178Y-Fas cells were pretreated with 100 μM ECH for 2 h, and ECH alone did not induce DNA fragmentation (Fig. 1*H*).

*ECH inhibits FasL-dependent DNA fragmentation mediated by perforin-negative CD4$^+$ CTL*

KLH-specific H-2$^d$-restricted CD4$^+$ CTL clone BK-1 cells are perforin-negative (33), and the killing pathway of this clone is exclusively dependent on FasL (29). BK-1 cells induced DNA

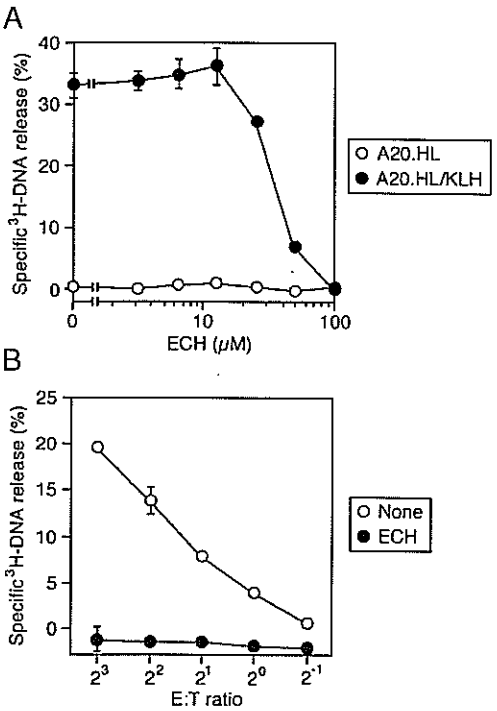


**FIGURE 2.** ECH inhibits FasL-based DNA fragmentation mediated by the CD4$^+$ CTL clone. *A*, [$^3$H]TdR-labeled A20.HL cells were pulsed with or without KLH (300 $\mu$g/ml) before assay. KLH-pulsed A20.HL (●) and nonpulsed A20.HL (○) cells were preincubated with serial dilutions of ECH for 1 h. The target cells were mixed with BK-1 cells (E:T cell ratio = 8), and then incubated for 4 h. *B*, [$^3$H]TdR-labeled KLH-pulsed A20.HL cells were preincubated with (●) or without (○) 100 $\mu$M ECH for 1 h. The target cells were mixed with different numbers of BK-1 cells and then incubated for 4 h. The radioactivity of fragmented DNA was measured. Data points represent the mean ± SD of triplicate cultures.

fragmentation in KLH-pulsed A20.HL cells, but not A20.HL cells without Ag (Fig. 2*A*). ECH markedly inhibited DNA fragmentation induced by BK-1 cells when KLH-pulsed A20.HL cells were pretreated with 50–100 $\mu$M for 1 h (Fig. 2).

To exclude the possibility that ECH pretreatment of target cells decreases CTL-target interaction, ECH-pretreated A20.HL cells were mixed with BK-1 cells, and resultant conjugate formation was analyzed by FACS (Fig. 3*A*). A brief centrifugation facilitated the formation of CTL-target conjugates. ECH did not influence conjugate formation at 50 $\mu$M. It should be noted that this concentration resulted in a profound inhibition of DNA fragmentation induced by BK-1 cells (Fig. 2*A*). As a slight reduction of CTL-target conjugates was observed when A20.HL cells were pretreated with 100 $\mu$M ECH, ECH might affect the interaction between CTL and target cells at higher concentrations.

### *ECH does not affect the components of lytic granules and granule exocytosis in CD8$^+$ CTL*

The H-2$^d$-specific CD8$^+$ CTL clone OE4 cells kill target cells via both the perforin-dependent pathway and the FasL-dependent pathway (18). As observed with BK-1 cells, ECH did not substantially prevent conjugate formation between OE4 and A20 cells up to 50 $\mu$M (Fig. 3*B*). Perforin and granzymes stored in lytic granules are released upon TCR activation and induce apoptosis in target cells. The cellular levels of perforin and granzymes were thus analyzed in OE4 cells exposed to ECH. In contrast to CMA that induced a marked reduction of perforin, ECH failed to decrease the cellular amount of perforin in OE4 cells (Fig. 4*A*). The enzyme activities of granzymes A and B in ECH-treated OE4 cells were also unimpaired (Fig. 4*B*). Stimulation of OE4 cells with plate-coated anti-CD3 Ab induced exocytosis of lytic granules into the culture medium, and ECH only marginally reduced granule exocytosis even at 50 $\mu$M (Fig. 4*C*). In our experimental system,

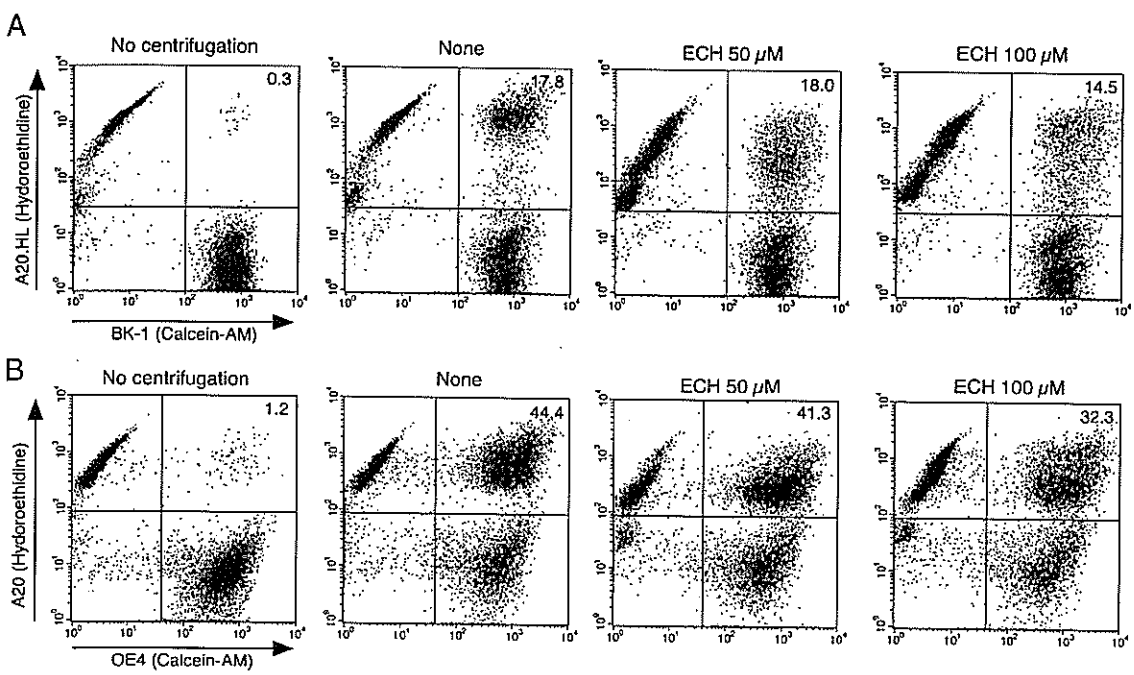


**FIGURE 3.** Effect of ECH on conjugate formation between CTL and target cells. *A*, Hydroethidine-stained A20.HL cells were treated with the indicated concentrations of ECH for 1 h, then mixed with calcein-AM-stained BK-1 cells in a single tube. The cells were either left untreated (*left panel*) or briefly centrifuged (*other panels*), and then incubated at 25°C for 30 min. *B*, Hydroethidine-stained A20 cells were treated with the indicated concentrations of ECH for 1 h, then mixed with calcein-AM-stained OE4 cells in a single tube. The cells were either left untreated (*left panel*) or briefly centrifuged (*other panels*), then incubated at 25°C for 30 min. Conjugate formation was analyzed by FACS.